

Department of Physics, Chemistry and Biology

Master's Thesis

# Search for Dark Matter in the Upgraded High Luminosity LHC at CERN

## Impact of ATLAS phase II performance on a mono-jet analysis

**Sven-Patrik Hallsjö**

Thesis work performed at Stockholm University

Linköping, June 4, 2014

LITH-IFM-A-EX--14/2863--SE



**Linköpings universitet**  
**TEKNISKA HÖGSKOLAN**

Department of Physics, Chemistry and Biology  
Linköping University  
SE-581 83 Linköping, Sweden



# **Search for Dark Matter in the Upgraded High Luminosity LHC at CERN**

## **Impact of ATLAS phase II performance on a mono-jet analysis**

**Sven-Patrik Hallsjö**

Thesis work performed at Stockholm University

Linköping, June 4, 2014

Supervisor:      **Docent Christophe Clément**  
                          FYSIKUM Stockholm University  
**Professor Magnus Johansson**  
                          IFM, Linköping University

Examiner:        **Professor Magnus Johansson**  
                          IFM, Linköping University





**Avdelning, Institution**  
Division, Department

Theoretical physics group  
Department of Physics, Chemistry and Biology  
SE-581 83 Linköping

**Datum**  
Date

2014-06-04

**Språk**  
Language

Svenska/Swedish  
 Engelska/English  
 \_\_\_\_\_

**Rapporttyp**  
Report category

Licentiatavhandling  
 Examensarbete  
 C-uppsats  
 D-uppsats  
 Övrig rapport  
 \_\_\_\_\_

**ISBN**  
—

**ISRN**  
LITH-IFM-A-EX--14/2863--SE

**Serietitel och serienummer**      **ISSN**  
Title of series, numbering      —

**URL för elektronisk version**

<http://urn.kb.se/resolve?urn=urn:nbn:se:liu:diva-XXXXXX>

**Titel**      Sökandet efter mörk materia i den uppgraderade hög luminositets LHC i CERN  
Title      Search for Dark Matter in the Upgraded High Luminosity LHC at CERN

**Undertitel**      Påverkan av ATLAS fas II prestanda på en mono-jet analys  
Subtitle      Impact of ATLAS phase II performance on a mono-jet analysis

**Författare**      Sven-Patrik Hallsjö  
Author

**Sammanfattning**  
Abstract

**Disclaimer: Abstract not yet completed.**

Something as an introduction:

The LHC at CERN is undergoing an upgrade to increase the center of mass energy for the colliding particles which means that new physical processes will be explored. One drawback of this is that it will be harder to isolate unique particle collisions since more and more collisions will occur simultaneously, so called pile-up.

One hope for the upgrade is that WIMP models of dark matter will be detected.

This thesis covers looking at effective operators which try to explain dark matter without adding new theories to the standard model or QFT.

Some results and a slight conclusion.

**Nyckelord**

Keywords

**Disclaimer: This not yet completed.**, ATLAS, Beyond standard model physics, CERN, Dark matter, Elementary particle physics, High energy physics, something, this is in mythesis.sty



## 4   **Abstract**

5   **Disclaimer: Abstract not yet completed.**

6   Something as an introduction:

7   The LHC at CERN is undergoing an upgrade to increase the center of mass en-  
8   ergy for the colliding particles which means that new physical processes will be  
9   explored. One drawback of this is that it will be harder to isolate unique parti-  
10   cle collisions since more and more collisions will occur simultaneously, so called  
11   pile-up.

12   One hope for the upgrade is that WIMP models of dark matter will be detected.

13   This thesis covers looking at effective operators which try to explain dark matter  
14   without adding new theories to the standard model or QFT.

15   Some results and a slight conclusion.



16 **Acknowledgments**

17 [REDACTED]

18 A big thank you to my family, fiancée and friends who have supported me through-  
19 out my education. A warm thank you to my friend Joakim Skoog who altered  
20 some of the images for me.

21 [REDACTED]

22 [REDACTED]

23 *Linköping, June 2014*  
24 *Sven-Patrik Hallsjö*



---

# Contents

## Notation

## 1 Introduction

1.1	Research goals . . . . .	2
1.2	Theoretical Background . . . . .	3
1.2.1	Quantum mechanics and quantum field theory . . . . .	3
1.2.2	Nuclear, particle and subatomic particle physics . . . . .	4
1.2.3	The standard model of particle physics . . . . .	4
1.2.4	Dark matter . . . . .	5
1.2.5	Effective field theory . . . . .	6
1.2.6	Search for WIMPS . . . . .	8
1.3	Experimental overview . . . . .	10
1.3.1	LHC . . . . .	10
1.3.2	ATLAS . . . . .	11
1.3.3	Coordinate system . . . . .	12
1.3.4	Reconstructing data . . . . .	12
1.3.5	Pile-up . . . . .	13
1.3.6	Mono-jet analysis . . . . .	13
1.3.7	Phase II high luminosity upgrade . . . . .	14
1.3.8	Monte Carlo simulation . . . . .	15

## 2 Validation of smearing functions

2.1	Smearing functions . . . . .	18
2.1.1	Electron and photon . . . . .	18
2.1.2	Muon . . . . .	18
2.1.3	Tau . . . . .	18
2.1.4	Jets . . . . .	18
2.1.5	Missing Transversal Energy . . . . .	18
2.2	Validation . . . . .	20
2.2.1	Method . . . . .	20
2.3	Results . . . . .	21
2.3.1	Electron and photon . . . . .	22
2.3.2	Muon . . . . .	23

58	2.3.3	Tau . . . . .	23
59	2.3.4	Jets . . . . .	24
60	2.3.5	Missing Transversal Energy . . . . .	25
61	2.4	Expected results . . . . .	26
62	2.5	Discussion . . . . .	28
63	2.5.1	Smearing independent on pile-up . . . . .	28
64	2.5.2	Comparison to expected results . . . . .	28
65	2.6	Conclusion . . . . .	29
66	<b>3</b>	<b>Evaluating dark matter signals</b>	<b>31</b>
67	3.1	Signal to background ratio . . . . .	32
68	3.1.1	Selection criteria . . . . .	32
69	3.1.2	Verifying background data . . . . .	32
70	3.1.3	Weight . . . . .	33
71	3.1.4	Figure of merit . . . . .	33
72	3.1.5	D5 operators . . . . .	34
73	3.1.6	Light vector mediator models . . . . .	34
74	3.2	Other selection criteria . . . . .	35
75	3.2.1	Criteria . . . . .	35
76	3.2.2	Verifying background data . . . . .	35
77	3.3	Mitigating the effect of the high luminosity . . . . .	35
78	3.4	Results . . . . .	36
79	3.4.1	Verifying background data . . . . .	36
80	3.4.2	Events . . . . .	36
81	3.4.3	Limit on $M^*$ . . . . .	38
82	3.4.4	Effect of pile-up on $M^*$ . . . . .	39
83	3.4.5	Previous results . . . . .	40
84	3.4.6	Limit on mediator mass . . . . .	40
85	3.4.7	Effect of pile-up on mediator mass . . . . .	41
86	3.5	Discussion . . . . .	42
87	3.5.1	Comparison to previous results . . . . .	42
88	3.5.2	Effect of the high luminosity . . . . .	42
89	3.6	Conclusion . . . . .	43
90	3.6.1	Limit on $M^*$ . . . . .	43
91	3.6.2	Limit on mediator mass . . . . .	43
92	<b>4</b>	<b>Results and Conclusions</b>	<b>45</b>
93	4.1	Validation of smearing functions . . . . .	45
94	4.2	Signal to background ratio . . . . .	46
95	4.2.1	Limit on $M^*$ . . . . .	46
96	4.2.2	Limit on mediator mass . . . . .	46
97	4.3	Other selection criteria and observables . . . . .	46
98	4.3.1	Limit on $M^*$ . . . . .	46
99	4.3.2	Limit on mediator mass . . . . .	46
100	4.4	Mitigating the effect of the high luminosity . . . . .	46
101	4.5	Recommendations to mitigate the effect of the high luminosity . . . . .	46

---

102	4.6 Suggestions for future research . . . . .	46
103	<b>A Datasets</b>	<b>49</b>
104	A.1 Background processes . . . . .	49
105	A.1.1 Validation . . . . .	49
106	A.1.2 Background to signals . . . . .	49
107	A.2 Signals . . . . .	50
108	A.2.1 Qcut . . . . .	50
109	A.2.2 D5 signal processes . . . . .	50
110	A.2.3 Light vector mediator processes . . . . .	50
111	<b>Bibliography</b>	<b>55</b>



# Notation

## NOTATIONS

Notation	Explanation
barn(b)	$1 \text{ barn}(b) = 10^{-24} \text{ cm}^2$
$\oplus$	$a \oplus b = \sqrt{a^2 + b^2}$ , $a \oplus b \oplus c = \sqrt{a^2 + b^2 + c^2}$

## ABBREVIATIONS

Abbreviation	Expansion
ATLAS	A large Toroidal LHC ApparatuS
CERN	Organisation européenne pour la recherche nucléaire <sup>1</sup>
CMS	Compact Muon Solenoid
CR	Control Region
LHC	Large Hadron Collider
MC	Monte Carlo
RMS	Root Mean Square
SM	the Standard Model of particle physics
SR	Signal Region
WIMP	Weakly Interacting Massive Particle
WIMPS	Weakly Interacting Massive ParticleS
QED	Quantum ElectroDynamics
QFT	Quantum Field Theory
QM	Quantum Mechanics

<sup>1</sup>Originally, Conseil Européen pour la Recherche Nucléaire



# 1

---

## Introduction

118 Discrepancies in measurements of the rotations of galaxies indicate the presence  
119 of a large amount of matter which interacts through gravity, though not elec-  
120 tromagnetically making it invisible to our telescopes. This matter is commonly  
121 referred to as dark matter. Since no known or hypothesised particle in the stan-  
122 dard model of particle physics can be used as a candidate for dark matter, this  
123 hints at the presence of new physics.

124 At the Organisation Européene pour la Recherche Nucléaire (CERN) focus now  
125 lies to discover any evidence of so called weakly interacting massive particles  
126 (WIMPS) which may be a candidate for dark matter. It is usually impossible to  
127 detect any interaction of dark matter candidates on the subatomic scale, however  
128 through looking at proposed interactions, searching for assumed decay channels  
129 and by investigating what is invisible to the detectors by using momentum con-  
130 servation it is hoped that signs will be found. Though to date, none have been  
131 found.

132 Both experiments and current theories now show that higher energies are re-  
133 quired at the LHC to be able to see any signs. This is why the LHC and all detectors  
134 are undergoing a vast upgrade program [1]. In this thesis focus will be on the last  
135 part of the upgrade due for completion in 2023, known as the high luminosity-  
136 LHC phase II upgrade; and also on the ATLAS detector. The method used in this  
137 thesis focuses on looking at data which emulate conditions at the upgraded LHC.

## 138 1.1 Research goals

139 This research took place at Stockholm University from January 7th until **when**?  
140 During the research period the following tasks were set up and performed/answered:

- 141 • Implement a C++ programme that loops over the collisions inside the signal  
142 and background datasets.
- 143 • For each collision retrieve the relevant observables (variables used to extract  
144 the signal over the background) and apply "smearing functions" to emulate  
145 the effect of the high luminosity on the observables.
- 146 • For both signal and background datasets, compare observables before and  
147 after smearing. What observables are the least/most affected?
- 148 • Implement selection criteria that selects the signal collisions efficiently while  
149 reduces significantly the background. In a first step the selection criteria  
150 should be taken from existing studies.
- 151 • Selection criteria can be evaluated and compared with each other using a  
152 figure of merit  $P$ , that measures the sensitivity of the experiment to the dark  
153 matter signal. Calculate  $P$  for the given selection criteria before and after  
154 smearing.
- 155 • What is the effect of the high luminosity (smearing) on the value of  $P$ ?
- 156 • Investigate other selection criteria and observables, to mitigate the effect of  
157 high luminosity. Use  $P$  to rank different criteria after smearing.
- 158 • Conclude on the effect of the high luminosity on the sensitivity for dark matter  
159 and possible ways to mitigate its effects using alternative observables  
160 and selection criteria.

## 161 1.2 Theoretical Background

### 162 1.2.1 Quantum mechanics and quantum field theory

163 In the beginning of the 20th century, some physical phenomena could not be ex-  
 164 plained by classical physics, for example the ultra-violet disaster of any classical  
 165 model of black-body radiation, and the photoelectric effect [2]. It was these phe-  
 166 nomena that led to the formulation of quantum mechanics (QM), where energy  
 167 transfer is quantized and particles can act as both waves and particles at the same  
 168 time [3].

169 Combining QM with classical electromagnetism proved harder than expected, col-  
 170 liding a photon(em-field) and an electron (particle/wave) is quite tricky. This  
 171 can be seen when trying to calculate the scattering between them both in a QM  
 172 schema. One idea that came from this was to explain them both in the same  
 173 framework, field theory. Also, trying to incorporate special relativity into QM  
 174 suggested a field description where space-time is described using the metric for-  
 175 malism from differential geometry. The culmination of both of these problems is  
 176 the first part of a Quantum field theory (QFT), Quantum electrodynamics (QED)  
 177 which with incredible precision explains electromagnetic phenomena including  
 178 effects from special relativity[4]. It is in this merging that antimatter was the-  
 179 orised, since it is a requirement for the theory to hold. After the discovery of  
 180 antimatter, the theory was set in stone. Since this the theory has been altered  
 181 somewhat to explain more and more experimental data. This is discussed more  
 182 in subsection 1.2.2 and subsection 1.2.3.

183 To be able to calculate properties in QFT one uses the Lagrangian formalism [5],  
 184 which gives a governing equation for the different physical processes. In general  
 185 the Lagrangian used for the Standard model is quite complicated, one can thus  
 186 focus on one of the different terms corresponding to a specific interaction. This  
 187 can be done to calculate the so called cross-section for a process, which is related  
 188 to the probability that that process will occur. A step to simplify the calcula-  
 189 tions is to use the so called Feynman diagrams, an example of which is given in  
 190 figure 1.1.

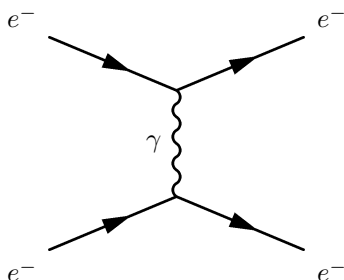


**Figure 1.1:** An example of a Feynman diagram explaining an electron-electron scattering using QED.

191 Through the figure, which comes with certain rules, and knowing what the major  
 192 process (in this case QED) one can calculate the cross-section [4]. It is this that is  
 193 needed to predict is one will be able to detect new particles.

## 1.2.2 Nuclear, particle and subatomic particle physics

Many could argue that these branches of physics started after Ernest Rutherford famous gold foil experiment [6], where he discovered that matter is composed of matter with a nucleus, a lot of empty space and electrons.

It was this that sparked the curiosity to see what the nucleus is made of and what forces govern the insides of atoms. After this, and the combination of the theoretical description given by QM, a lot more has been discovered and still more has been predicted. The newest of these is of course the Higgs particle, which was predicted through QFT and then discovered by the ATLAS and the CMS experiments at CERN [7].

The discovered particles are often divided into different groups depending on the fundamental particles that build them up. For instance, particles build up of three quarks are known as hadrons. Particles with an integer spin are known as bosons whereas half-integer particles are known as fermions.

## 1.2.3 The standard model of particle physics

The standard model of particle physics, referred to simply as the standard model (SM), is the particle zoo which tries to categorize all the particles and that have been discovered experimentally. QFT explains the interactions between these particles and it has also predicted several particles by including symmetries [6]. Regarding SM, Gauge bosons are the force carriers for the different forces, quarks are the and leptons are the fundamental blocks that we know of so far. The difference between the later two is if they interact via the strong force or not.

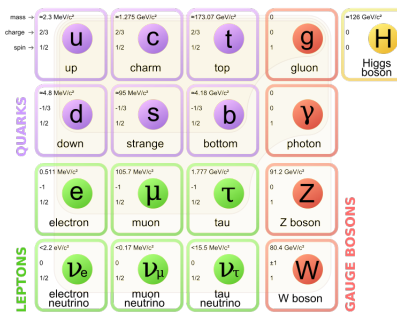


**Figure 1.2:** The standard model of particle physics where the three first columns represent the so called generations, starting with the first. [8].

SM is today the pinnacle of particle physics and can be used to explain almost everything that occurs around us. There are however some problems [9]:

- There is no link between gravity and the SM.
- Asymmetry between matter and antimatter can not be fully explained.
- No dark matter candidate!
- No explanation that can contain dark matter.

222 In this thesis focus lies with dark matter, some more introduction to possible  
 223 dark matter and different candidates in extensions to SM are explained in subsection  
 224 1.2.4.

### 225 1.2.4 Dark matter

226 Dark matter is among other things, the name given to the solution to the discrepancies  
 227 of galactic rotations.

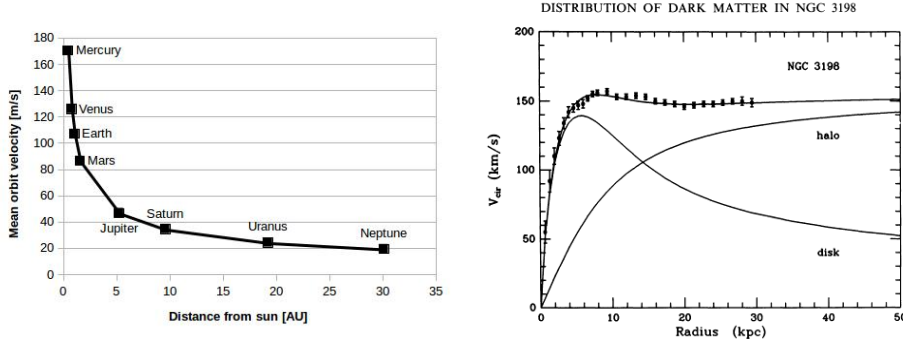
228 To explain this, focus on matter in a galaxy which are rotating around the center  
 229 of the galaxy. Through Newtons law of gravity and the centrifugal force one can  
 230 calculate the rotation speed dependent on the distance to the center of the galaxy.  
 231 Since one of these forces is attractive and the other repulsive, if the matter is in  
 232 a stable orbit around the galactic center (which they are) they must be equal and  
 233 give us an expression for the speed depending on the distance. Newtons law can  
 234 be written as the following:

$$F_{Gravitational} = G \frac{Mm}{r^2} = G_M \frac{m}{r^2} \quad F_{Centrifugal} = m \frac{V^2}{r} \quad (1.1)$$

235 where G is the gravitational constant, M the mass of the centre object, m the mass  
 236 of the matter, r the distance between the two and V is the rotation speed. It has  
 237 been simplified using  $G_M$  since all matter orbits the same galactic center. Setting  
 238 the equations in (1.1) results in:

$$G_M \frac{m}{r^2} = m \frac{V^2}{r} \Leftrightarrow V^2 = \frac{G_M}{r} \Rightarrow V = \sqrt{\frac{G_M}{r}} \propto \frac{1}{\sqrt{r}} \quad (1.2)$$

239 where the speed is assumed to be positive and  $\propto$  means proportional. Through  
 240 these simple calculations it shown that the rotation speed should decrease with  
 241 and increased distance. The same reasoning can be applied to our solar system  
 242 where this is the case figure 1.3a. The relation in these units is  $V = \frac{107}{\sqrt{r}}$  where  
 243 107 can be used in (1.2) to calculate the mass of the sun. However when looking  
 244 at galaxies, even when taking into account that one has to see the galaxies as a  
 245 mass distribution and that the above is only true when outside of the inner mass  
 246 half, this is not the case! In figure 1.3b experimental data can be seen from the  
 247 galaxy NGC3198 with a fitted curve which does not decrease with the distance  
 248 but is instead constant. This is the discrepancy which is solved by postulating  
 249 the existence of dark matter. After this the big question arises, what could this  
 250 dark matter consist of? What is known so far lies in the name. It is called dark  
 251 since there is no electromagnetic interaction and matter since it has gravitational  
 252 interaction. This means that it can not be made up of any baryonic matter or  
 253 anything in the Standard Model apart from neutrinos. The main interest of this  
 254 thesis and also the main contributor to the rotational discrepancies is known as  
 255 cold dark matter. This is due to the matter having a low speed, thus low kinetic  
 256 energy, and have a high particle mass (In the GeV scale) [9, 12, 13]. This means  
 257 however that neutrinos can not be a candidate, thus dark matter can not be made  
 258 out of any standard model particles. There are several ideas to detected dark  
 259 matter, [9]



(a) *Rotation speed of planets in our solar system. Since the distance is quite small on an astronomical scale, there is no sign of dark matter. Based on data from [10].*

(b) *Rotation speed of mater in NGC3198 with a curve fitting and three different models, if only a dark model halo existed, if there was no dark matter and the correct, if both exist [11].*

**Figure 1.3:** Different rotation curves, both for planets in our solar system and matter in the NGC3198 galaxy.

- Ordinary matter interacting with ordinary matter can produce dark matter, known as production. Which is the processes that occurs at particle accelerators.
- Dark matter interacting with ordinary matter can produce dark matter, known as direct detection.
- Dark matter interacting with dark matter can produce ordinary matter, known as indirect detection.

In this thesis the focus lies with production. There are several theories how to detect dark matter in proton-proton collisions such that occur at the LHC at CERN this is covered more in subsection 1.2.6.

## 1.2.5 Effective field theory

In quantum field theory the objective is usually to find the part of the Lagrangian which explains a type of interaction, known as the operator of the interaction and also to find the probability amplitude (cross-section) for a certain interaction. For complicated processes it is easier to employ certain conditions so that the small scale phenomena are simplified and the whole picture understood. This is known as using an effective field theory and the concept is explained in figure 1.4. The operator can be found through assuming the possible interactions and using the effective field theory [4]. The cross-sections can be found through the Feynman diagrams as described in subsection 1.2.1.

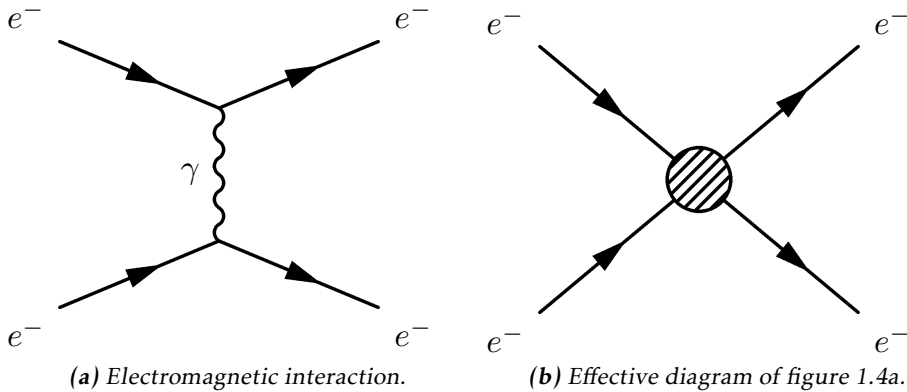


**Figure 1.4:** Feynman diagram of an electron-electron scattering, both as an ordinary diagram and as its effective theory version, where the details are hidden in the blob.

In this thesis the same effective field theory as in Refs. [12, 14] will be considered. The WIMP (usually denoted  $\chi$ ) is assumed to be the only particle in addition to the standard model fields. It is assumed that an even number of  $\chi$  must be in every coupling. It is assumed that the mediator exists is heavier than the WIMPS, meaning that their interactions are in higher order terms of the effective field theory and thus not included in the operators. For simplicity, the WIMPS are assumed to be SM singlets, thus invariant under SM gauge transformations, and the coupling to the Higgs boson is neglected.

<sup>288</sup> The operators used in this thesis are assumed to be quark bilinear operators on  
<sup>289</sup> the form  $\bar{q}\Gamma q$  where  $\Gamma$  is a  $4 \times 4$  matrix of the complete set,

$$\Gamma = \{1, \gamma^5, \gamma^\mu, \gamma^\mu \gamma^5, \sigma^{\mu\nu}\} \quad (1.3)$$

This will dictate how the operators are written, more of why this is done can be found in [4, 12, 14].

This defines an effective field theory of the interaction of singlet WIMPs with hadronic matter. It is an approximation which will break down when the mediator mass is close to the mass of the WIMP. The condition for this is derived in [14] and gives:

$$M > 2m_\chi \quad (1.4)$$

where  $m_\chi$  is the mass of the WIMP and  $M$  is the mass of the mediator particle. There is also the requirement that:

$$M \lesssim 4\pi M_* \quad (1.5)$$

where  $M_*$  is the energy scale where the effective theory is no longer a good approximation.

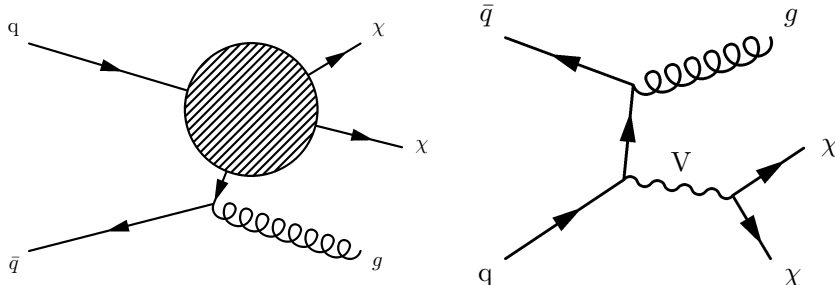
300 In this work, WIMPS are assumed to be Dirac fermions (half integer spin and is  
 301 not its own antiparticle).

302 In table 1.1 the operators which are integrated out via the effective field theory  
 303 and are of interest in this thesis are given.

Name	Initial state	Type	Operator
D1	qq	scalar	$\frac{m_q}{M_*^3} \bar{\chi} \chi \bar{q} q$
D5	qq	vector	$\frac{1}{M_*^2} \bar{\chi} \gamma^\mu \chi \bar{q} \gamma_\mu q$
D8	qq	axial-vector	$\frac{1}{M_*^2} \bar{\chi} \gamma^\mu \gamma^5 \chi \bar{q} \gamma_\mu \gamma^5 q$
D9	qq	tensor	$\frac{1}{M_*^2} \bar{\chi} \sigma^{\mu\nu} \chi \bar{q} \sigma_{\mu\nu} q$
D11	gg	scalar	$\frac{1}{4M_*^3} \bar{\chi} \chi \alpha_s (G_{\mu\nu}^a)^2$

**Table 1.1:** Table based on discussion in [13].

304 Where D denotes that the WIMPS are assumed to be Dirac fermions. These can all  
 305 be described using figure 1.5a.



**(a)** Effective Feynman diagram explaining the D-operators. **(b)** Feynman diagram describing the vector mediator model.

**Figure 1.5:** Feynman diagrams describing the signal models used in this thesis.

306 Another model which is considered is a vector mediator model which is described  
 307 by figure 1.5b.

## 308 1.2.6 Search for WIMPS

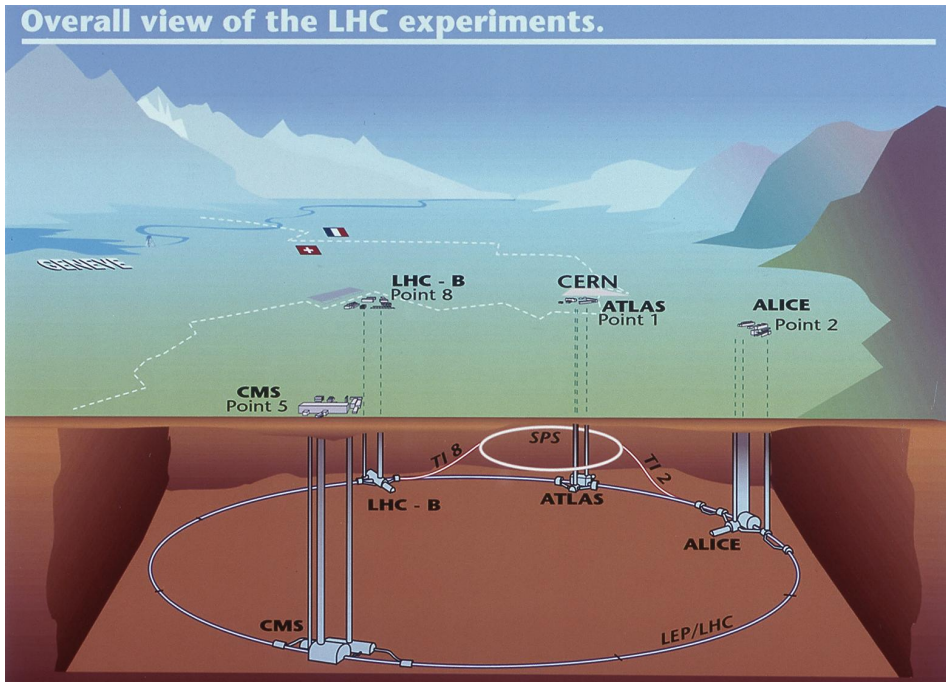
309 The search for WIMPS is based on a mono-jet analysis which is described in sub-  
 310 section 1.3.6. This method revolves around a high energetic jet which arises from  
 311 the gluon from figure 1.5b and momentum missing from the energy conservation.

- 312 This means that something has happened which the detectors can not detect. If  
313 the models from subsection 1.2.5 can explain the missing energy, then a model  
314 for WIMPS has been found.
- 315 Since the search for WIMPS at the LHC is based on looking at the missing energy,  
316 not actual detection, the experiment can not establish if a WIMP is stable on a  
317 cosmological time scale and thus if it is a dark matter candidate [13]. This means  
318 that if a candidate is found, it may still not be the dark matter that is needed to  
319 explain the cosmological observations.
- 320 The different theories discussed in subsection 1.2.5 require some process in which  
321 quarks and anti-quarks are produced. At ATLAS they have looked at proton-  
322 proton collisions, in which they are produced, with 8 TeV center of mass energy  
323 with out finding any excess of mono-jet events. This is why it is very interesting  
324 that the LHC is undergoing a upgrade that will allow higher energy levels, see  
325 subsection 1.3.7. With this the processes can be given higher energy and thus the  
326 produced particles can be comprised of higher mass.

## 327 1.3 Experimental overview

### 328 1.3.1 LHC

329 The large hadron collider (LHC) is a particle accelerator located at CERN near  
 330 Geneva in Switzerland, see figure 1.6. The accelerator was built to explore physics  
 331 beyond the standard model and to make more accurate measurements of stan-  
 332 dard model physics. Before it was shut down for an upgrade in 2012 it was able  
 333 to accelerate two proton beams to such a velocity that each proton in them had  
 334 an energy of 4 TeV which gives a center of mass energy,  $\sqrt{s} = 8$  TeV. The proton  
 335 beam is comprised of bunches of protons with enough spacing that bunch col-  
 336 lisions can happen independent of each other. Apart from the energy, the rate at  
 337 which the accelerator produces a certain process can be calculated through the  
 338 instantaneous luminosity. For the LHC the instantaneous luminosity was  $10^{34}$   
 339  $\text{cm}^{-2}\text{s}^{-1}$  [15] or  $10\text{nb}^{-1}\text{s}^{-1}$  where 1 barn(b) =  $10^{-24} \text{ cm}^2$ .



340 **Figure 1.6:** Figure showing the LHC and the different detector sites[16].

341 The instantaneous luminosity, often just denoted luminosity, can be defined in  
 342 different ways depending on how the collision takes place. For two collinear  
 intersecting particle beams it is defined as:

$$\mathcal{L} = \frac{f k N_1 N_2}{4\pi \sigma_x \sigma_y} \quad (1.6)$$

343 where  $N_i$  are the number of protons in each of the bunches,  $f$  is the frequency  
 344 at which the bunches collide ,  $k$  the number of colliding bunches in each beam,  
 345 and  $\sigma_x$  ( $\sigma_y$ ) is the horizontal (vertical) beam size at the interaction point. Since  
 346 the instantaneous luminosity increases quadratically with more protons in each  
 347 bunch, increasing the number of protons would be a good strategy to increase  
 348 the instantaneous luminosity. However aside from the difficulties to create and  
 349 maintain a beam with more particles, a large  $N_i$  increases the probability for  
 350 multiple collisions per bunch crossing, referred to as pile-up. Pile up will be a  
 351 key aspect which is described more in subsection 1.3.5.

352 The expected number of events can be calculated by using the instantaneous lu-  
 353 minosity through the following:

$$N = \sigma \int \mathcal{L} dt \equiv \sigma \mathcal{L} \quad (1.7)$$

354 where  $\mathcal{L}$  is the integrated luminosity and  $\sigma$  is the cross section which is often  
 355 measured in barn. The integrated luminosity is a measurement of total number  
 356 of interactions that have occurred over time. Before the LHC was shut down  $\mathcal{L}$   
 357 was  $20.8 \text{ fb}^{-1}$ .

358 The cross section, as explained in subsection 1.2.1, is a measure of the effective  
 359 surface area seen by the impinging particles, and as such is expressed in units  
 360 of area. The cross section is proportional to the probability that an interaction  
 361 will occur. It also provides a measure of the strength of the interaction between  
 362 the scattered particle and the scattering center. Further details can be found in  
 363 reference [17].

### 364 1.3.2 ATLAS

365 As seen in figure 1.6, there are several detectors at the LHC. One of these is  
 366 ATLAS which is a general purpose detector that uses a toroid magnet. Its goal  
 367 is to observe several different production and decay channels. The detector is  
 368 composed of three concentric sub-detectors, the Inner detector, the Calorimeters  
 369 and the Muon spectrometer [18].

370 The Inner detectors main task is to detect the tracks of the particles. It also mea-  
 371 sures the position of the initial proton-proton collision.

372 The Calorimeters, electromagnetic and hadronic, are used to calculate the energy  
 373 contained in the different particles. The electromagnetic detects particles which  
 374 are charged, and the hadronic those which are neutral.

375 The Muon spectrometer is used to detect signs of muons, which will simply pass  
 376 through the other detectors without leaving a trace. It also calculates the energy  
 377 and momentum of the muons.

378 The neutrinos escape the ATLAS experiment without being detected, and in this  
 379 thesis it is assumed that WIMPS pass through all the detectors without leaving  
 380 any trace.

### 381 1.3.3 Coordinate system

382 The coordinate system of ATLAS, seen in figure 1.7 is a right-handed coordinate  
 383 system with the x-axis pointing towards the centre of the LHC ring, and the z-axis  
 384 along the tunnel/beam (counter clockwise) seen from above. The y-axis points up-  
 385 ward. The origin is defined as the geometric center of the detector. A cylindrical  
 386 coordinate system is also used for the transversal plane,  $(R, \phi, Z)$ . For simplicity  
 387 the pseudorapidity of particles from the primary vertex is defined as:

$$\eta = -\ln(\tan \frac{\theta}{2}) \quad (1.8)$$

388 where  $\theta$  is the polar angle (xz-plane) of the particle direction measured from  
 389 the positive z-axis.  $\eta$  is through this definition invariant under boosts in the z-  
 390 direction.

391 It is quite common to calculate the distance between particles and jets in the  
 392  $(\eta, \phi)$  space,  $d = \sqrt{(\Delta\eta)^2 - (\Delta\phi)^2}$ .

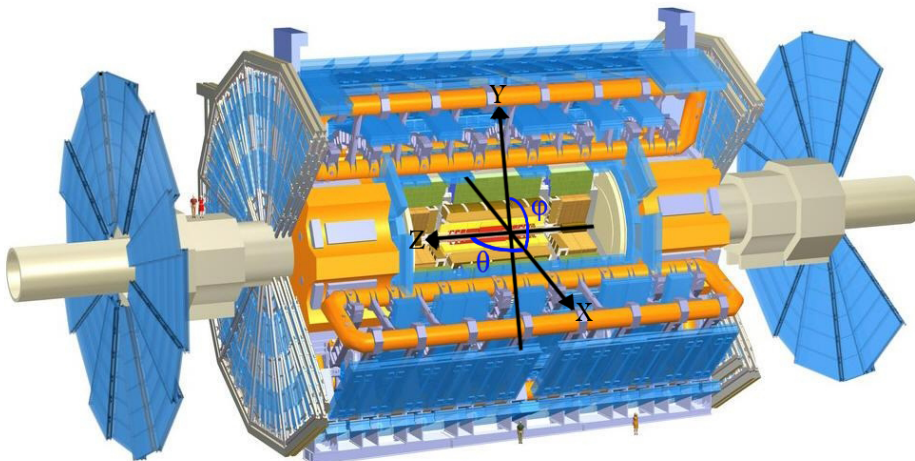


**Figure 1.7:** The ATLAS detector and the definition of the orthogonal Cartesian coordinate system. Image altered from[19]

### 393 1.3.4 Reconstructing data

394 To be able to compare the simulated data to real data it is important to include  
 395 effects of the detectors. This is done using so called smearing functions which try  
 396 to emulate the reconstruction of data.

397 The reconstruction process of data [18] is based on what response is given from  
 398 the detectors. It is affected by pile-up and the energy of that which is detected.  
 399 This process is not specifically used in the thesis, however the smearing functions  
 400 are discussed in section 2.1.

### 401 1.3.5 Pile-up

402 Pile-up is the phenomena that several proton-proton collisions occur simultaneously.  
 403 The number of pile-up is defined as the average number of proton-proton  
 404 collisions that occur per bunch crossing per second. It is denoted as  $\langle \mu \rangle$ .  $\mu$  can  
 405 be calculated by adjusting a Poisson distribution to fit the curve created by the  
 406 number of interactions per bunch crossing at a given luminosity. When this is  
 407 done  $\mu$  will be the mean value of the Poisson distribution.

### 408 1.3.6 Mono-jet analysis

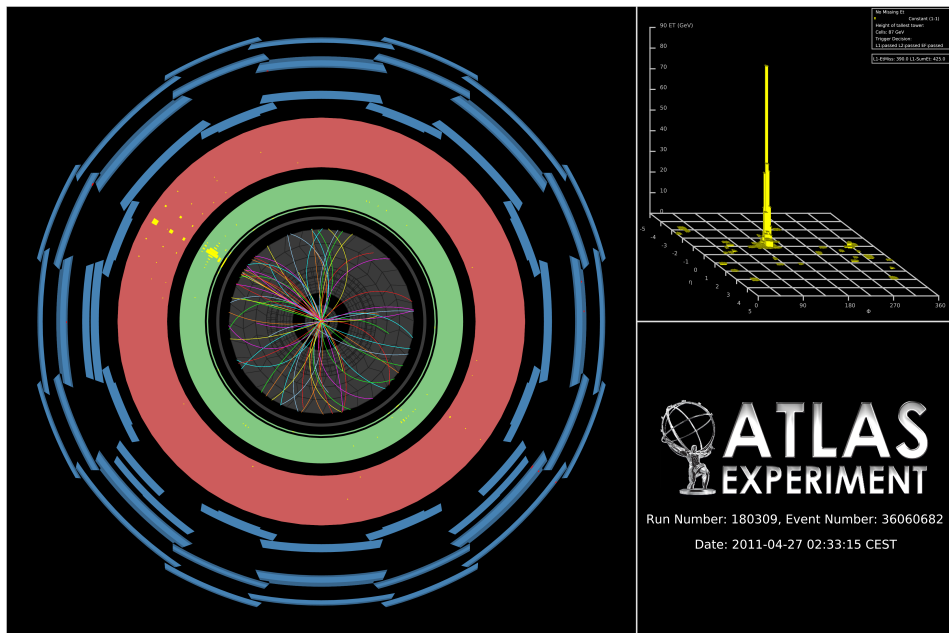


**Figure 1.8:** Image of an actual mono-jet event recorded by the ATLAS experiment [20].

409 When measuring the transversal energy one can in some interactions find incon-  
 410 sistencies, such as jets that are in excess in one direction. In figure 1.8 one can see  
 411 a high energetic jet which gives an excess of transversal energy in one direction  
 412 after the collision. Since there is no balancing jet there must be transverse energy  
 413 that is not detected, denoted  $E_T^{Miss}$ , since it was close to zero before the collision.  
 414 This gives an indication that there energy to balance this that simply can not be  
 415 detected. This could for instance be neutrinos or the sign of a new particle.

416  $E_T^{Miss}$  is the modulus of the  $E_T^{Miss}$  vector which is defined as:

$$E_T^{\vec{M}iss} = -\sum E_T^{\vec{jet}} - \sum E_T^{\vec{Electron}} - \sum E_T^{\vec{\mu}on} - \sum E_T^{\vec{T}au} - \sum E_T^{\vec{\gamma}on} \quad (1.9)$$

417 Jets are hadrons which travel in the same direction and are usually created from

hadronization of a quark or a gluon in a collision. Usually jets are composed of a lot of energetic hadrons.

Since the jets are created from quarks or gluons, measuring a jet results in more information about the collision.

There are two main classes of events, signal and background. The signal corresponds to events that would arise from one of the processes in subsection 1.2.5. However to know that the missing energy is sign of the signal then one must understand all the other components that could contribute to the missing energy. Also there must be an excess of missing energy from what is expected from the background.

The background comprises of standard model processes that can mimic the mono-jet signature.

### 1.3.7 Phase II high luminosity upgrade

At the moment, the whole LHC is undergoing a step by step upgrade program which will be finalized around 2022-2023, denoted the high luminosity upgrade, or HL-upgrade. The upgrade consists of different stages, meaning that the upgrade will halt for periods so that experiments can take place. In figure 1.9 one can see

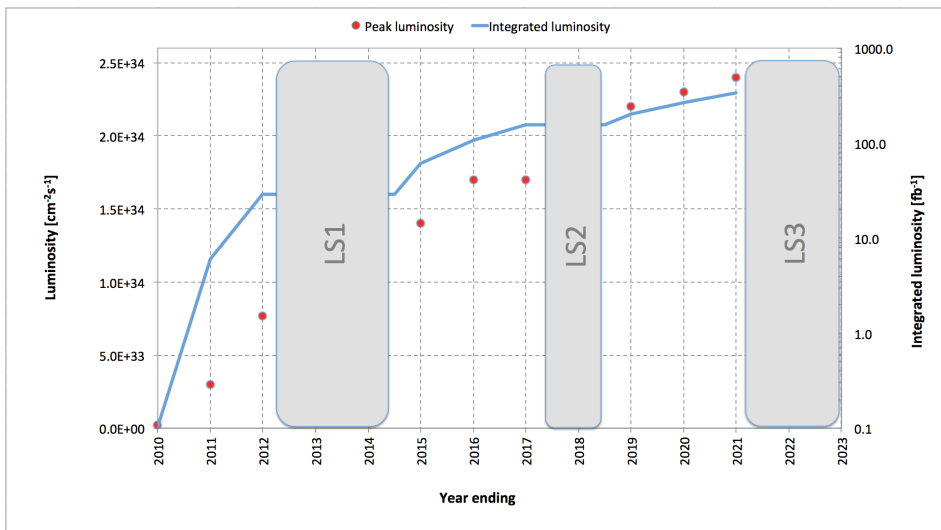


**Figure 1.9:** A graph showing the upgrading timetable with the instantaneous luminosity, denoted luminosity, and integrated luminosity expected in the different stages.

the three proposed upgrades. The period before LS1 is denoted phase 0, after LS1 and before LS2 phase I and after LS3 phase II.

LS1 is the upgrade which will take the LHC to its designed performance.

- 438 LS2 will take the LHC to the ultimate designed instantaneous luminosity.  
 439 LS3 which is the focus of this thesis, will increase the instantaneous luminosity  
 440 even more. Though for this to happen a modification of the whole LHC  
 441 must be done, instead of just an upgrade and maintenance as before.

442 The following is expected for the experiments done after phase II:

Entity	Expected	Last run (2012)
Instantaneous luminosity	$\mathcal{L} \sim 50 \text{ nb}^{-1} \text{s}^{-1}$	$\mathcal{L} \sim 10 \text{ nb}^{-1} \text{s}^{-1}$
Integrated luminosity	$\mathcal{L} = 1000 - 3000 \text{ fb}^{-1}$	$\mathcal{L} = 20 \text{ fb}^{-1}$
Pile-up	$\langle \mu \rangle = 140$	$\langle \mu \rangle = 20$
Center of mass energy	$\sqrt{s} = 14 \text{ TeV}$	$\sqrt{s} = 8 \text{ TeV}$

**Table 1.2:** Expected running values for the Phase II HL-upgraded LHC with older values for comparison [21].

443 Where it should be noted that the integrated luminosity indicates the total amount  
 444 of data which will be collected after the upgrade is completed before the next up-  
 445 grade takes place.

### 446 1.3.8 Monte Carlo simulation

- 447 As mentioned before, in this thesis only emulated data has been used. This data  
 448 is created by using a Monte Carlo (MC) simulation of the background processes  
 449 and the expected signal. To do this a program called MadGraph is used.  
 450 MadGraph [22] starts with Feynman diagrams and then generates simulated events  
 451 based on lots of different parameters.  
 452 PYTHIA [23] is a package which adds the correct description of jets to MadGraph  
 453 by including hadronization. The correct description of pile-up comes from other  
 454 ATLAS software.  
 455 The tool to access all this data and analyse it a tool called ROOT, which is used  
 456 for programming high energy physics related tools [24].



# 2

---

## Validation of smearing functions

459 A full detector simulation of the ATLAS detector based on the GEANT [25] pro-  
460 gram makes it possible to obtain the expected detector responses to electrons,  
461 muons, tau leptons, photons ( $\gamma$ ) and jets of hadrons. However these simulations  
462 are extremely time-consuming and require a lot of computing power. Also at the  
463 present time only a limited set of these simulations exists for the ATLAS phase II  
464 upgrade.

465 In this thesis a different strategy is used. Instead of performing a full detector  
466 simulation the observed particles from the event generator, which simulates the  
467 proton-proton collisions, are smeared by using random numbers following reso-  
468 lution functions specific to each type of particle. These emulate how the detector  
469 and the reconstruction is affected by the increased luminosity and the pile-up  
470 which comes with this.

471 The resolution functions or smearing functions are the official functions devel-  
472 oped from previous studies [1, 26] by the ATLAS collaboration for the study of  
473 the ATLAS phase II upgrade. The key feature of those studies was that the di-  
474 rection of the momenta is unaffected and that only jets and  $E_T^{Miss}$  are affected by  
475 pile-up. Since this was confirmed in previous studies it was not incorporated into  
476 the smearing functions as discussed more in section 2.1.

477 Since part of this thesis work was to take the official ATLAS smearing functions  
478 and apply the smearing to each particle, it was important to check that the en-  
479 ergy and momenta resolutions of the smeared objects were consistent with the  
480 expected values. Thus in this chapter the energy and momenta resolutions are  
481 measured after applying the smearing to some simulated processes and the re-  
482 sulting resolutions are compared with the expected values.

## 483 2.1 Smearing functions

484 These smearing functions are designed so that they take into account the effi-  
 485 ciency of the different detectors, limitations from how they are constructed as  
 486 well as their dependence on pile-up. They also take into account how all this  
 487 varies depending on the measured entries energy or momenta.

488 Terminology:

- 489 • Data before smearing, simulated data, is denoted as data at a truth level or  
 490 truth data.
- 491 • Data after smearing, which is comparable to what is measured is denoted  
 492 as reconstructed or reco data as discussed in subsection 1.3.4.

### 493 2.1.1 Electron and photon

494 The identification of electrons relies on finding an isolated electron track and  
 495 a pattern in the calorimeter compatible with an electron shower. Pile-up will  
 496 affect the electrons by decreasing the efficiency to identify an electron because of  
 497 the increased number of tracks. However for the identified electrons the energy  
 498 resolution will be close to that without pile-up.

499 The electron and photon have the same smearing since they are both detected in  
 500 a similar way.

### 501 2.1.2 Muon

502 The identification of muons relies on isolated tracks in the inner detector being  
 503 matched with information in the muon system. Since the muon system is the  
 504 outer most detector seen from the collision point it is unaffected by the false  
 505 detection effects of pile-up.

### 506 2.1.3 Tau

507 Tau is detected similarly to electron and photon. In this thesis all tau processes  
 508 are assumed to be at 3 prong. Where prong refers to the different amount of  
 509 tracks from which they were reconstructed. This in turn means that the effect of  
 510 pile-up will be worse compared to an electron as a triplet must be found in an  
 511 increased number of tracks.

### 512 2.1.4 Jets

513 The largest effect of pile-up is to add additional jets in the ATLAS detector. These  
 514 additional jets contribute to additional energy deposited inside the existing jets  
 515 and to  $E_T^{Miss}$ .

### 516 2.1.5 Missing Transversal Energy

517  $E_T^{Miss}$ , the missing transversal energy, which was discussed in subsection 1.3.6,  
 518 and defined in (1.9) is calculated by knowing that there should be energy conser-

519 vation in the collision. It is comprised of different parts, one from neutrinos, one  
520 from errors in the other measurements and one from new physics. It should be  
521 affected by pile-up as described above.

## 522 2.2 Validation

523 To validate the smearing functions a comparison with Ref. [26] was made where  
 524 the standard deviation, depending on the energy or momentum value of an entity,  
 525 was given, see section 2.4. This is performed using the simulated processes listed  
 in table 2.1.

**Table 2.1:** Different processes from where data has been taken. Each sample is a simulation of a physical process, the simulation names can be found in appendix A

Particle	Process
Electron	$W \rightarrow e\nu$
Muon	$W \rightarrow \mu\nu$
Tau	$W \rightarrow \tau\nu$
$\gamma$	$\gamma + \text{Jet sample}$
Jets	Jet sample
$E_T^{\text{Miss}}$	$Z \rightarrow \nu\nu + \text{Jet sample}$

526

### 527 2.2.1 Method

528 The energy and momentum resolutions are obtained for each type of particle by  
 529 comparing the values before and after smearing.

530 This is done by looking at the reco data for a given slice at a truth energy or mo-  
 531 mentum value. Since the smearing functions takes a lot into account the match  
 532 will not be a fine line as seen in figure 2.3b.

533 By fitting a Gaussian curve to this data will then result in the standard deviation  
 534 which is used in the validation. The standard deviation is also known as the  
 535 resolution of the data and will be denoted  $\sigma$ .

536 This resolution is then compared to previous results, [26].

537 To get enough statistics enough data must be available for a given truth energy  
 538 or momenta and the analysis must be specific enough to only look at a narrow  
 539 enough interval around this point.

540 Step by step method

- 541 • Take a MC sample with a given particle, i.e electrons.
- 542 • Choose a slice of electron which have a truth energy of a given value (75  
   543 GeV for electrons).
- 544 • Plot the smeared electron energy for this slice of truth energy. Given for  
   545 electrons and photons in figure 2.1.
- 546 • For this distribution of smeared energy, fit a Gaussian distribution and cal-  
   547 culate the sigma value of this Gaussian.
- 548 • Compare this sigma, which is the calculated resolution to the expected res-  
   549 olution given from the smearing functions.

## 550 2.3 Results

- 551 As discussed above, the method was to plot the data against its smeared counter-  
552 part and through this determine  $\sigma$  to see if it conforms to the expected values.
- 553 Only one energy value is shown for simplicity, though the comparison was done  
554 for different energy values.
- 555 The average number of pile-up is fixed at 60 as a benchmark unless anything else  
556 is stated.
- 557 As the comparison, figure 2.4, figure 2.1, figure 2.2 and figure 2.5 are divided  
558 depending on the different  $\eta$  values.
- 559 All results are summarized in table 2.5.

### 2.3.1 Electron and photon

Since these interact very similarly in the detector, their smearing functions are identical. The slice value represents at which value of unsmeared energy or momentum this smearing occurs.

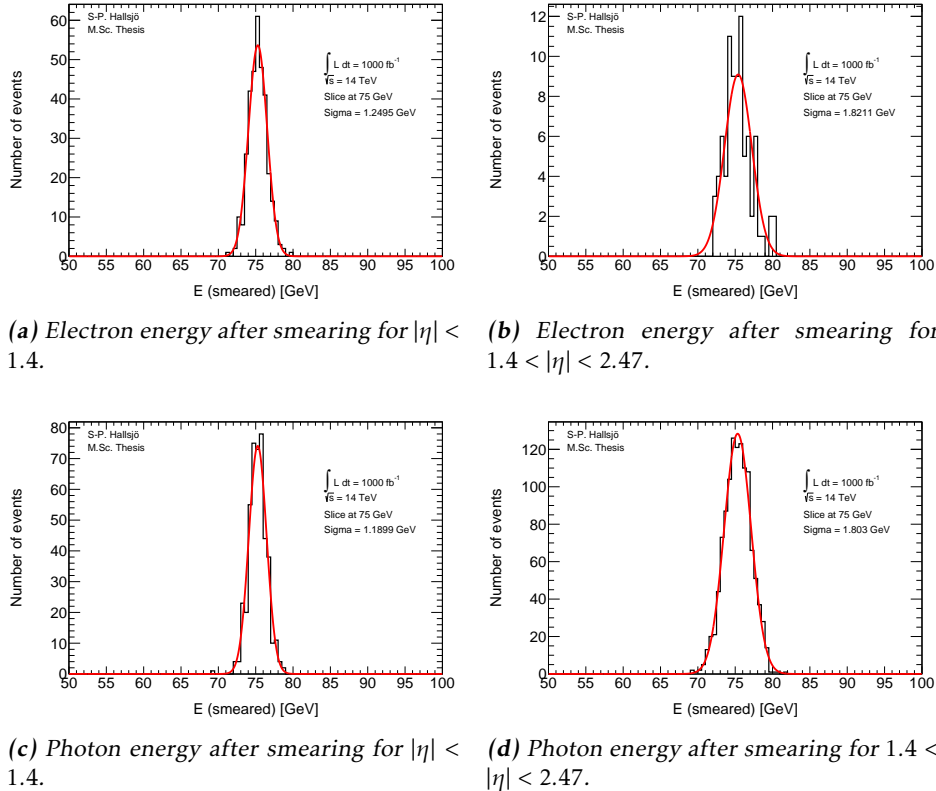
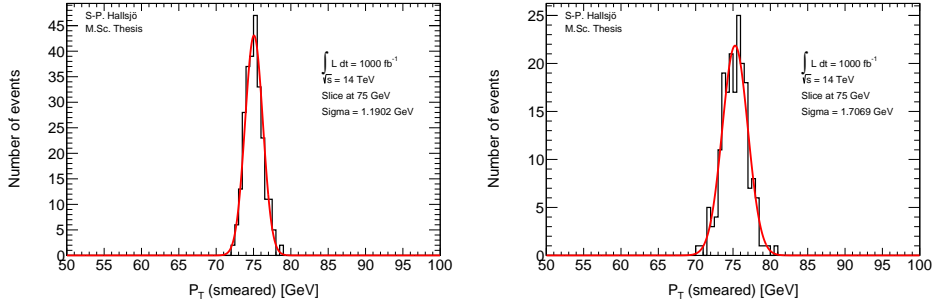


**Figure 2.1:** Photon and electron energy after smearing.

### 564 2.3.2 Muon

565 Since muons are shielded from the effects of pile-up only efficiency and detector  
 566 limitations affect the smearing.

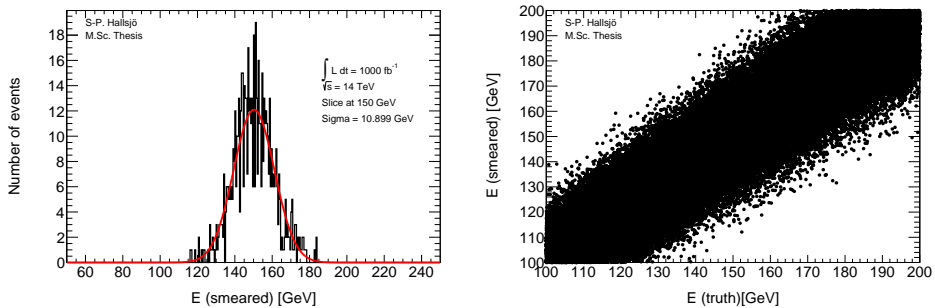


(a) Muon momenta after smearing for  $|\eta| < 1.05$ . (b) Muon momenta after smearing for  $1.05 < |\eta|$ .

**Figure 2.2:** Muon momenta after smearing.

### 567 2.3.3 Tau

568 As described in subsection 2.1.3 tauons are detected similarly to electrons and  
 569 photons. Thus the plots should look similarly to those in the previous subsection  
 570 apart from the slice being at 150 GeV. In figure 2.3a the Gaussian fit (red) and the  
 571 data (black) are given for tau detected through 3 prong. In figure 2.3b smeared  
 572 versus truth energy is shown.



(a) Tau energy after smearing.

(b) Tau energy vs smeared.

**Figure 2.3:** Tau energy after smearing and energy vs smearing.

### 2.3.4 Jets

Jets as described in subsection 1.3.6, are hadronic showers. The smearing functions are divided into four different regions depending on the angle  $\eta$ .

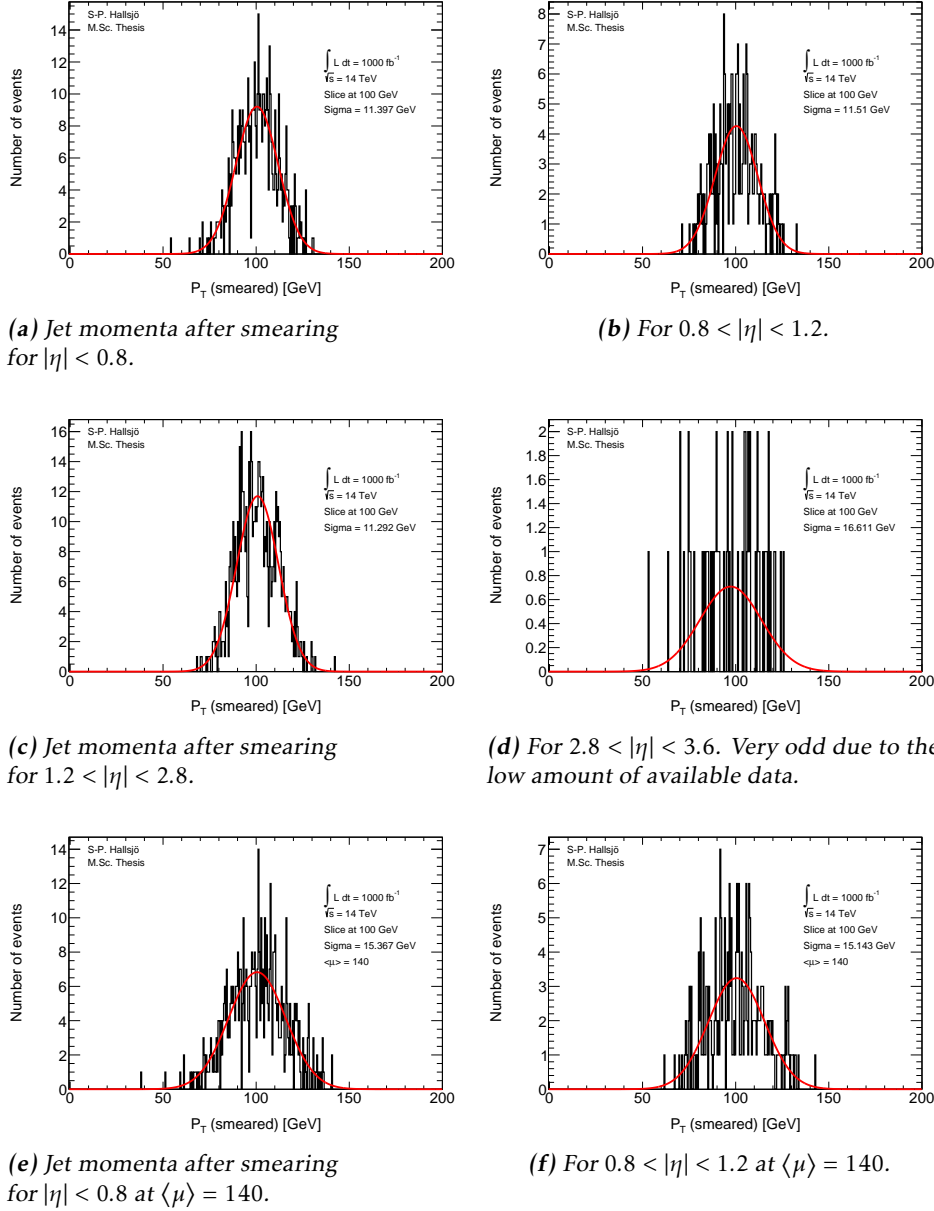


**Figure 2.4:** Jet momenta after smearing.

### 576 2.3.5 Missing Transversal Energy

577 The figures in this subsection are, compared to the above, given as absolute smear-  
 578 ing, thus at 0 it represents that the energy is unsmeared, compared to the others  
 579 where the slice value represents the unsmeared.

580 Here the  $E_T^{Miss}$  is projected down to the x- and y-axis, since these are the transver-  
 581 sal axes, to be smeared.

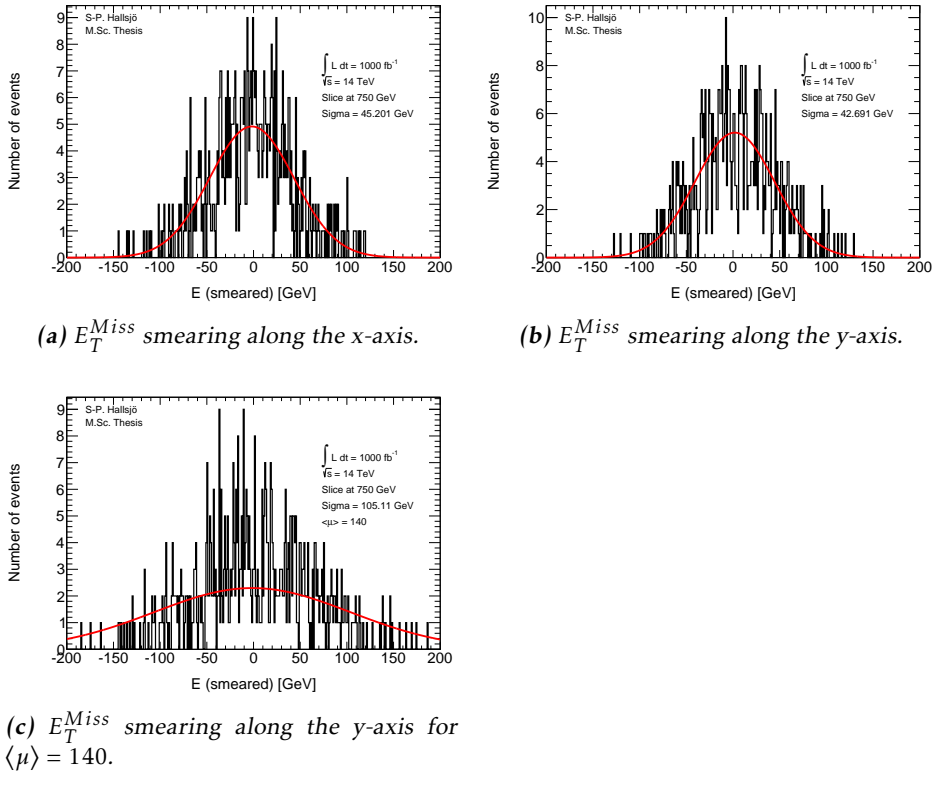


**Figure 2.5:**  $E_T^{Miss}$  smearing plots

## 582 2.4 Expected results

583 Since the leptons and photons are all detected by fitting detectors responses to  
 584 different tracks, meaning that the effect of pile-up should be that there are more  
 585 track to match, but it should not affect which ones are matched. The indepen-  
 586 dence of pile-up for leptons and photons is backed up in previous research, for  
 587 instance [1, 27].

588 To validate the smearing code, comparisons were made with [26] which gave the  
 589 following formulation for the expected  $\sigma$ :

Observable	Absolute $\sigma$
Electron & photon	$\sigma = 0.3 \oplus 0.1\sqrt{E(GeV)} \oplus 0.01E(GeV),  \eta  < 1.4$ $\sigma = 0.3 \oplus 0.15\sqrt{E(GeV)} \oplus 0.015E(GeV), 1.4 <  \eta  < 2.47$
Muon momentum	$\sigma = \frac{\sigma_{id}\sigma_{ms}}{\sigma_{id} \oplus \sigma_{ms}}$ $\sigma_{id} = P_T(a_1 \oplus a_2 P_T)$ $\sigma_{ms} = P_T(\frac{b_0}{P_T} \oplus b_1 \oplus b_2 P_T)$
Tau energy	$\sigma = (0.03 \oplus \frac{0.76}{\sqrt{E(GeV)}})E(GeV)$ , for 3 prong.
Jet momentum	$\sigma = P_T(GeV)(\frac{N}{P_T} \oplus \frac{S}{\sqrt{P_T}} \oplus C)$ where $N = a(\eta) + b(\eta)\mu$
$E_T^{Miss}$	$\sigma = (0.4 + 0.09\sqrt{\mu})\sqrt{\sum E(GeV) + 20\mu}$

**Table 2.2:** Expected absolute  $\sigma$  where the parameters are given for muons in table 2.3 and for jets in table 2.4. Functions take from [26].

	$a_1$	$a_2$	$b_0$	$b_1$	$b_2$
$ \eta  < 1.05$	0.01607	0.000307	0.24	0.02676	0.00012
$ \eta  > 1.05$	0.03000	0.000387	0.00	0.03880	0.00016

**Table 2.3:** Parameters used in the muon smearing function taken from [26].

$ \eta $	a	b	s	C
0-0.8	3.2	0.07	0.74	0.05
0.8-1.2	3.0	0.07	0.81	0.05
1.2-2.8	3.3	0.08	0.54	0.05
2.8-3.6	2.8	0.11	0.83	0.05

**Table 2.4:** Parameters used in the jet smearing function taken from [26].

Process	$\sigma$ [GeV]	Expected $\sigma$
Electron low $\eta$	$1.25 \pm 0.05$	1.18
High $\eta$	$1.82 \pm 0.14$	1.74
Photon low $\eta$	$1.19 \pm 0.04$	1.18
High $\eta$	$1.80 \pm 0.04$	1.74
Muon low $\eta$	$1.19 \pm 0.05$	1.50
High $\eta$	$1.71 \pm 0.09$	2.18
Tau	$10.90 \pm 0.31$	10.34
Jet low $\eta$	$11.40 \pm 0.35$	11.60
$\langle \mu \rangle = 140$	$15.37 \pm 0.47$	15.77
Mid low $\eta$	$11.51 \pm 0.52$	11.94
$\langle \mu \rangle = 140$	$15.14 \pm 0.68$	15.95
Mid high $\eta$	$11.29 \pm 0.31$	10.94
High $\eta$	$16.61 \pm 1.53$	13.50
$E_T^{Miss}$ x-axis	$45.20 \pm 1.35$	48.45
$E_T^{Miss}$ y-axis	$42.69 \pm 2.28$	48.45
$\langle \mu \rangle = 140$	$105.11 \pm 12.24$	87.28

**Table 2.5:**  $\sigma$  values.

- 590 • Where the given  $\sigma$  is still the absolute.
- 591 • Where the large difference between calculated and expected  $\sigma$  for Muons  
592 and  $E_T^{Miss}$  is explained by incorrectly calculated errors in  $\sigma$ .

## 593 2.5 Discussion

### 594 2.5.1 Smearing independent on pile-up

595 From the validation done it was interesting to note that the smearing functions  
596 were created from previous studies, [1, 27], which had shown that leptons and  
597 photons are not affected by pile-up. This may seem incredible however it be-  
598 comes quite logical when one understands how the detectors work. To be able to  
599 detect particles the detectors must detect an excess of energy which comes from  
600 a particle passing through. This should not be distorted by an increased pile-up.  
601 The amount of particles passing through will of course increase, but the detec-  
602 tions should be unaffected as well as the recreation of the events. However with  
603 the same logic it makes sense that jets and  $E_T^{Miss}$  are quite affected since they  
604 are combined of several parts, either hadronic particles or by all the transversal  
605 missing energy.

606 Another interesting part is how the effect diminishes with and increasing energy.  
607 As seen above, and through the the formula, for the high energies which were of  
608 interest here the effect is minimal.

### 609 2.5.2 Comparison to expected results

610 One of the major problems in the comparison was to get the significance of the  
611 Gaussian fit to be calculated correctly. The tool ROOT has a lot of different fea-  
612 tures which made this task somewhat difficult. Also since this is a statistical  
613 property there is a statistical fluctuation in the result.

614 Another was to retrieve the correct values from the paper, [26], since it was un-  
615 clear if the values given were absolute or scale dependent. This has now been  
616 corrected in a new version of the paper.

## 617 **2.6 Conclusion**

618 The smearing functions work as intended within 5.8 sigma, however when using  
619 a test box and averaging the sigmas one ends up with half of this for the extreme  
620 cases, muons and  $E_T^{Miss}$ y-axis.



# 3

---

## Evaluating dark matter signals

623 **Disclaimer: All data provided is still a work in progress and may be subject to  
624 change before the final version.**

625 The main goal of the thesis is to investigate if certain dark matter signals can  
626 be detected after the high luminosity upgrade. One immediate worry is that the  
627 background will be large in comparison to the signal, making the signal undetectable.  
628

629 The signal models are given in appendix A along with the background models.  
630 The different models were discussed in part in subsection 1.2.5 and some more  
631 in this chapter.

632 This thesis focus on using a luminosity at  $1000 \text{ fb}^{-1}$  and a center of mass energy  
633 at 14 TeV. The reco data is created using a pile-up rate,  $\langle \mu \rangle = 140$  as expected  
634 during phase II.

635 Each of these has been evaluated in different signal regions and the detectability  
636 has been evaluated using a statistical P-value. This process has been performed  
637 at different pile-up values.

## 638 3.1 Signal to background ratio

### 639 3.1.1 Selection criteria

640 For different purposes different selection criteria or regions are used. These are a  
 641 set of criteria specified to enhance the area of interest. For instance, if simulating  
 642 a specific signal one wants to find as many ways as possible to diminish the back-  
 643 ground. This so that when searching experimentally, the signal will be easier to  
 644 detect.

645 These can be quite general cuts, there are only some things to take into consider-  
 646 ation.

- 647 • If experimental, what limitations are set by the detectors? Are there some  
 648 criteria already?
- 649 • If simulated, is there some criteria set in the generator?
- 650 • Are there criteria which must be set since there is to much uncertainty in  
 651 the data? or a large effect of pile up?

### 652 3.1.2 Verifying background data

653 To verify that the background data was correct it was compared with Ref. [28]  
 654 in which the center of mass energy is 8 TeV and the luminosity is  $10 \text{ fb}^{-1}$ . Since  
 655 the luminosity is not  $1000^{-1}$  as used in this thesis the expected values from the  
 656 paper scaled up with a factor 100 to be comparable.

657 Somewhat unexpectedly a center of mass energy at 8 TeV required the cross-  
 658 sections to be a factor 4 lower than the cross-sections at 14 TeV. **How do I ref-**  
 659 **erence the cross-section?**

The signal regions used in the article were the following:

---

Selection Criteria		
Jet veto, require no more than 2 jets with $p_T > 30 \text{ GeV}$ and $ \eta  < 4.5$		
Lepton veto, no electron or muon		
Leading jet with $ \eta  < 2.0$ and $\Delta\phi(\text{jet}, E_T^{\text{miss}}) > 0.5$ (second-leading jet)		
signal region	SR3p	SR4p
minimum leading jet $p_T$ (GeV)	350	500
minimum $E_T^{\text{miss}}$ (GeV)	350	500

---

660 **Table 3.1:** The signal regions from Ref. [28].

661 The article had in total four signal regions, unfortunately since the simulated  
 662 events used in this thesis are filtered before the analysis only the two highest  
 663 regions are comparable. This can be seen in subsection 3.4.1 in table 3.3.

664 **3.1.3 Weight**

665 A weight is used to normalize different types of data so that they can be compared.  
 666 In thesis the following is used:

$$667 \text{weight} = \frac{\mathcal{L}\sigma}{N_{Raw}} \quad (3.1)$$

667 where  $N_{Raw}$  is number of events expected at the luminosity that was set to create  
 668 the data, compared to  $\mathcal{L}$  which is the luminosity at which the data is compared  
 669 and  $\sigma$  is the cross-section.

670 **3.1.4 Figure of merit**

671 To be able to evaluate different signal regions and different signal models, a figure  
 672 of merit  $p$  is used. The value  $p$  is the probability for an assumed hypothesis  
 673 to be correct, thus a good signal region will yield a low value. The assumed  
 674 hypothesis is that the background and its fluctuations is measured over the signal  
 675 plus background.

676 Assuming the expected number of background events are  $B \pm \sigma_B$  where  $\sigma_B$  is the  
 677 quadratic sum of the statistical error from Monte Carlo, the statistical error from  
 678 the control region (CR) and the systematic errors. The expected number of signals  
 679 is  $S$ , assumed without fluctuation.

680 If no uncertainty in  $B$  or  $S$  is assumed, then the number of expected events,  $N$ , in  
 681 the signal region should follow a Poisson distribution as such:

$$682 P(N|S+B) = \frac{e^{-(S+B)}(S+B)^N}{N!} \quad (3.2)$$

683 However since there is an uncertainty in the background, the probability distribution  
 684  $P(N|S+B)$  must be convoluted with a Gaussian function:

$$685 G(N_B|B, \sigma_B) = \frac{1}{\sigma_B \sqrt{2\pi}} e^{-\frac{(N_B-B)^2}{2\sigma_B^2}} \quad (3.3)$$

where  $N_B$  is the expected number of background events. The convolution is done  
 using  $N_B$  as  $N$  resulting in the total probability density function:

$$686 F(N|S+B, \sigma_B) = P(N|S+N_B)*G(N_B|B, \sigma_B) = \\ = \int_{-\infty}^{\infty} P(N|N_B - (S+B))G(N_B|B, \sigma_B)dN_B \quad (3.4)$$

687 This leads to the probability of the signal plus background fluctuation to  $B$  events  
 688 being obtained by summing the probability function from  $N=0$  to  $N=B$ .

$$689 p = \sum_{i=0}^B \int_{-\infty}^{\infty} P(i|N_B - (S+B))G(N_B|B, \sigma_B)dN_B \quad (3.5)$$

In this thesis, two different models of the error in the background  $\sigma_B$  are used. Both models are based on Ref. [28]. As described in the beginning of this subsection the error is calculated as:

$$\sigma_B = \text{Statistical error from MC} \oplus \text{Statistical error in CR} \oplus \text{Systematic error}$$

- The statistical error from MC has been neglected since there is no way of estimating it for the used data.
- The statistical error from background CR has been assumed to decrease with the increased luminosity,  $\frac{30}{380} \frac{\sqrt{L_{old}}}{\sqrt{L_{new}}}$
- The systematic error has been given two different values, from the article:  $\frac{30}{380}$  or fixed at 0.02.
- All this results the total error being used as either, 0.0793411 or 0.0215018.

### 3.1.5 D5 operators

As described in the introduction subsection 1.2.5, one of the signals is modelled using the D5 operator. In this thesis two different scenarios were used, one at a dark matter mass of 50 GeV and one at 400 GeV.

Each of these models are modelled with a mass suppression scale, denoted  $M^*$ , which is strongly correlated to the cross-section of the process.

One property which is of interest is to calculate how large  $M^*$  can be so that the signal is still detectable over the background processes. These results are given in subsection 3.4.3.

### 3.1.6 Light vector mediator models

As described in the introduction subsection 1.2.5, the other signal model is a vector mediator model. In this thesis these signals have two different width scenarios and a number of different mediator mass scenarios. In addition to this there are, as with the D5 operator two different dark matter mass scenarios.

#### What is width?

The models which are detectable are given in subsection 3.4.6.

## 709 3.2 Other selection criteria

### 710 3.2.1 Criteria

711 To be able to compare signal results to previous papers new signal regions were  
 712 devised. It was also discovered that the requirement of no electrons was to harsh  
 713 for the signal models. Because of this new signal criteria were devised.

---

#### Selection Criteria

Jet veto, require no more than 2 jets with  $p_T > 30\text{GeV}$  and  $|\eta| < 4.5$

Lepton veto, no electron or muon.

The electron veto is defined:  $\Delta R(jet^{lead}, electron^{lead}) \geq 0.4$  and  
 $electron^{lead} p_T > 20\text{GeV}$  removed.

Leading jet with  $|\eta| < 2.0$  and  $\Delta\phi(jet, E_T^{Miss}) > 0.5$  (second-leading jet)

signal region	SR1	SR1p	SR2	SR3	SR4
minimum leading jet $p_T$ (GeV)	350	500	600	800	1000
minimum $E_T^{Miss}$ (GeV)	350	500	600	800	1000
signal region	SRa		SRb	SRc	SRd
minimum leading jet $p_T$ (GeV)	350		350	350	350
minimum $E_T^{Miss}$ (GeV)	350		600	800	1000

Table 3.2: The new signal regions

### 714 3.2.2 Verifying background data

715 To make sure that the altered electron veto still produces results comparable with  
 716 [28] a comparison was made again. This can be seen in subsection 3.4.1 in ta-  
 717 ble 3.4.

## 718 3.3 Mitigating the effect of the high luminosity

719 As discussed in subsection 2.5.1 the effect of pile-up should be minimal in the  
 720 high energy regions which are of interest in this thesis.

721 Mention that the effect is on a trigger level, that the lowest SR will be lost.

722 Even though this was envisioned as the primary focus of the thesis, it was shown  
 723 that the effect of pile-up is minute for these high signal regions. Thus the focus  
 724 was shifted to perform a more in-depth mono-jet analysis of different DM signal  
 725 models.

## 726 3.4 Results

### 727 3.4.1 Verifying background data

728 In table 3.3 a comparison has been made. It can be seen that the simulated events  
 729 and expected events coincide on all accounts apart from  $W \rightarrow \tau\nu$ ,  $W \rightarrow \mu\nu$  and  
 730 thus the total as well. **This can be explained by better separation of  $\mu, \tau$  and**  
 731 **missing energy.** Tau can not be reconstructed as jets in the code, they can in  
 732 reality!

733 Here used truth data as to not be effected by pile-up.

Process	SR3p	Expected SR3p	SR4p	Expected SR4p
$Z \rightarrow \nu\nu$	140298	152000	25250.3	27000
$W \rightarrow \tau\nu$	40700.8	37000	5861.74	3900
$W \rightarrow e\nu$	11229	11200	1506.58	1600
$W \rightarrow \mu\nu$	13727.1	15800	1872.32	4200
Total background	205955	218000	34491	36700

**Table 3.3:** Comparison of the simulated and expected events from [28] with  $\mathcal{L} = 1000\text{fb}^{-1}$ , cross-sections corresponding to  $\sqrt{s} = 8\text{TeV}$  and using the same electron veto.

Process	SR1	Expected SR1	SR1p	Expected SR1p
$Z \rightarrow \nu\nu$	147009	152000	26734	27000
$W \rightarrow \tau\nu$	44727.7	37000	6543.82	3900
$W \rightarrow e\nu$	17964	11200	2470.46	1600
$W \rightarrow \mu\nu$	14285.7	15800	1971.87	4200
Total background	223986	218000	37720.2	36700

**Table 3.4:** Comparison of the simulated and expected events from [28] with  $\mathcal{L} = 1000\text{fb}^{-1}$ , cross-sections corresponding to  $\sqrt{s} = 8\text{TeV}$  and using a modified electron veto.

### 734 3.4.2 Events

735 Give a table with the number of events for signals and background in all signal  
 736 regions both truth and reco.

737 The below is only for truth, must create new code to write it for reco.

738 Have a table with the number of signal and bkg ground events for the different  
 739 SR where the signal then is given at  $M^* 1\text{ GeV}$  for a good comparison.

740 Same tables as above but at reco.

Process	SRa/SR1	SRb	SR2	SRc	SR3	SRd	SR4
D5 mDm=50 $Q_{cut} = 200$	50410.4	434.012	0	0	0	0	0
M*=1TeV $Q_{cut} = 400$	53242.1	10018.1	4934.73	159.539	0	22.0054	0
$Q_{cut} = 600$	26210.6	25958.1	25284.7	12767.2	10749.7	5199.47	4391.35
Total signal	129863	36410.1	30219.4	12926.8	10749.7	5221.48	4391.35
Z $\rightarrow \nu\nu$	604479	58613.9	42656.5	11383.4	8423.89	2842.85	2110.55
W $\rightarrow \tau\nu$	154140	10678.5	7807.06	1788.16	1307.89	385.861	295.124
W $\rightarrow e\nu$	61771.6	3961.35	2890.39	653.918	485.485	152.221	109.887
W $\rightarrow \mu\nu$	49114.3	3051.61	2357.17	498.995	379.201	108.086	90.9721
Total background	869505	76305.4	55711.2	14324.5	10596.5	3489.02	2606.54

**Table 3.5:** Signal and background events for truth data in the signal regions.

Process	SRa/SR1	SRb	SR2	SRc	SR3	SRd	SR4
D5 mDm=50 $Q_{cut} = 200$	41968.9	564.215	0	0	0	0	0
M*=1TeV $Q_{cut} = 400$	52235.9	13131.8	4126.01	275.068	0	22.0054	0
$\langle\mu\rangle = 140$ $Q_{cut} = 600$	26090	25065.8	23893	13477.1	9978.04	5482.88	4130.4
Total signal	120295	38761.9	28019	13752.2	9978.04	5504.88	4130.4
Z $\rightarrow \nu\nu$	553735	71613.2	39104.6	13145.1	7680.99	3139.89	1932.33
W $\rightarrow \tau\nu$	156023	14500.3	7741.1	2174.02	1282.23	467.433	275.877
W $\rightarrow e\nu$	58873.9	5177.33	2705.75	789.925	447.655	175.639	106.284
W $\rightarrow \mu\nu$	47800.6	4030.7	2298.63	617.889	380.102	138.71	89.1707
Total background	816433	95321.6	51850	16727	9790.98	3921.67	2403.66

**Table 3.6:** Signal and background events for reco data with  $\langle\mu\rangle = 140$  in the signal regions.

741 **Disclaimer: The thesis is not completed after here.**

### 742 3.4.3 Limit on $M^*$

743 The mass suppression scale.

744 Give at 1000fb-1 and with 14 TeV cross-sections. And for the different signal  
745 regions. Refer to  $M^*$  explained in subsection d5. subsection 3.1.5

746 For the new signal regions: **Include a table of the limits for truth and Reco.**

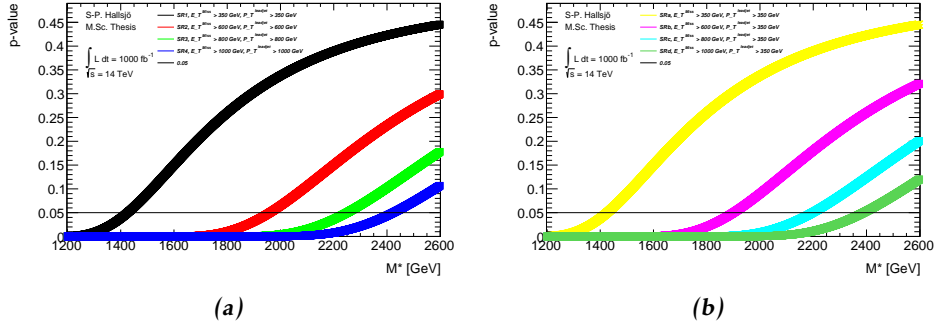


**Figure 3.1:** On a truth level error model 0.02.

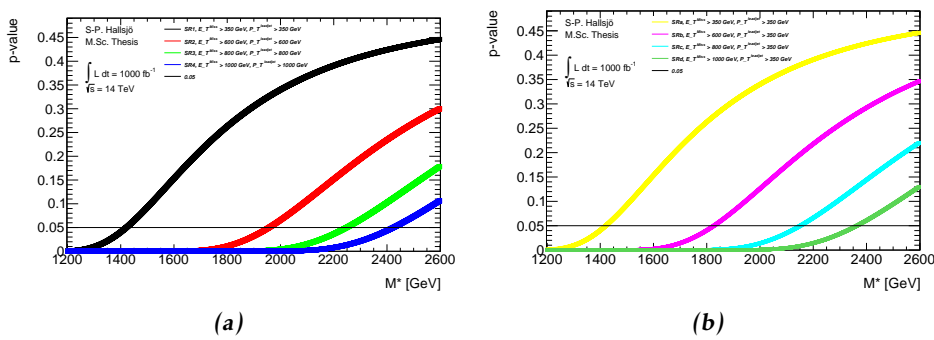


**Figure 3.2:** On a reco level error model 0.02.

Signal region	Mass suppression scale Truth data	Reco data
SR1	1425	1420
SR2	1960	1957
SR3	2249	2248
SR4	2423	2423
SRA	1425	1421
SRb	1900	1827
SRc	2197	2152
SRd	2389	2363

**Table 3.7:** Mass suppression scales in GeV given for the 0.02 error model.

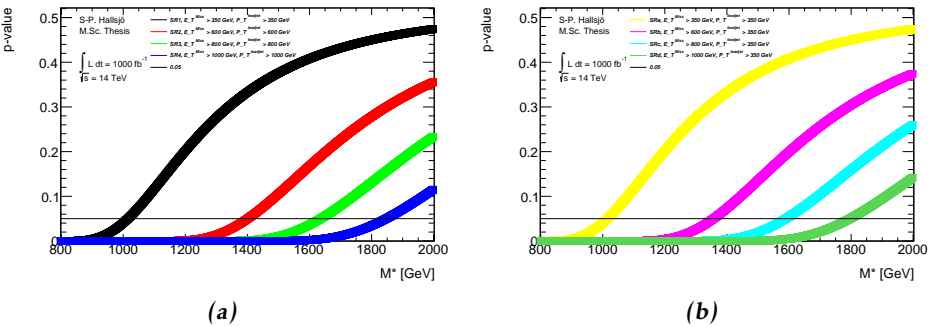


**Figure 3.3:** On a truth level error model 0.10.

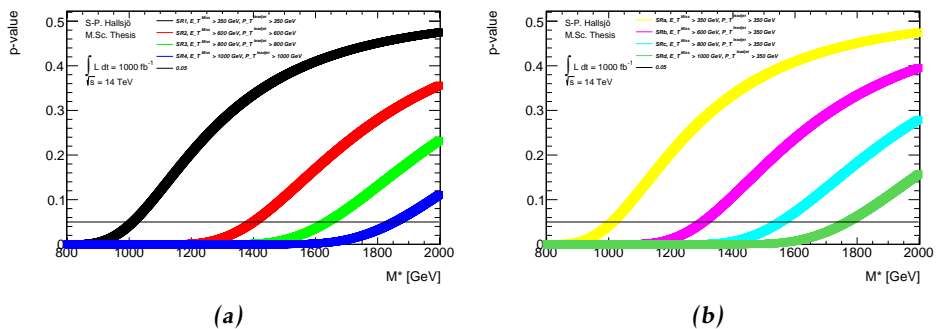


**Figure 3.4:** On a reco level error model 0.10.

#### 3.4.4 Effect of pile-up on $M^*$

747 Hardly any effect. 10 % or in that vicinity.

Signal region	Mass suppression scale Truth data	Reco data
SR1	1015	1012
SR2	1400	1400
SR3	1636	1637
SR4	1846	1854
SRa	1015	1012
SRb	1356	1303
SRc	1589	1553
SRd	1796	1768

**Table 3.8:** Mass suppression scales in GeV given for the 0.10 error model.

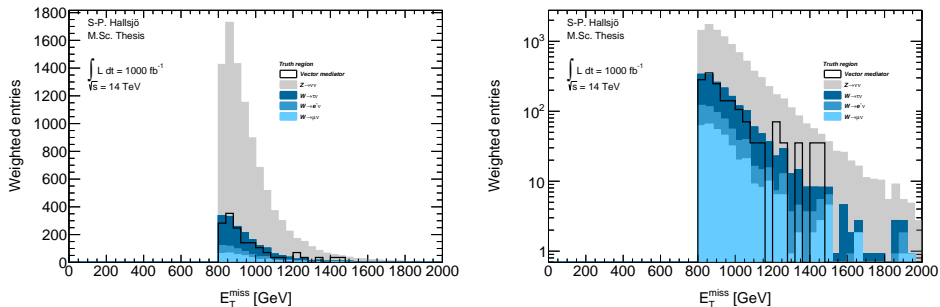
### 3.4.5 Previous results

750 10fb paper. Preliminary not that much better results for 1000fb-1 and 14TeV.

751 The whole discussion with Steven and David.

### 3.4.6 Limit on mediator mass

753 Are there previous results? Signal vs background plot in normal and log scale for  
 754 one of the vector mediator models, to be able to evaluate all the different models  
 755 the so called p-value was used in different signal regions. Below are two figures  
 756 showing one of the vector mediator models in SR3.



(a) Signal on background plot for  $E_T^{\text{miss}}$  on  
 757 reco level in SR3. (b) The same as a) with log scale on the y-axis

**Figure 3.5:** Signal on background plot to illustrate the a general plot.

757 To set a limit on the mediator mass the p-value was calculated in different sig-  
 758 nal regions for the different signal models with different mediator mass. This  
 759 resulted in the following plot:

760 **3.4.7 Effect of pile-up on mediator mass**

761 Check the different cases for reco and truth to see what happens.

## 762 **3.5 Discussion**

### 763 **3.5.1 Comparison to previous results**

### 764 **3.5.2 Effect of the high luminosity**

**765 3.6 Conclusion****766 3.6.1 Limit on  $M^*$** **767 3.6.2 Limit on mediator mass**



768

# 4

769

---

## Results and Conclusions

770 **Disclaimer: This chapter not yet completed.**

### 771 **4.1 Validation of smearing functions**

772 Have some discussion.

773 Result they appear to work as expected, the reference paper was a bit unclear, I  
774 leave my writing as a better reference.

## 775 **4.2 Signal to background ratio**

### 776 **4.2.1 Limit on M\***

### 777 **4.2.2 Limit on mediator mass**

## 778 **4.3 Other selection criteria and observables**

### 779 **4.3.1 Limit on M\***

### 780 **4.3.2 Limit on mediator mass**

## 781 **4.4 Mitigating the effect of the high luminosity**

## 782 **4.5 Recommendations to mitigate the effect of the 783 high luminosity**

784 Keep to a higher energy region, or signal region.

## 785 **4.6 Suggestions for future research**

786 With more time, search for new signal regions, the only solution now for the HL  
787 is to go up in energy. Since none of the other parameters (eta,phi etc) seem to be  
788 altered these can not be used. Is there something that has been overlooked?

789 Test the effect of pile-up for lower signal regions? See if the effect is as great as  
790 predicted.

791 Explore other theoretical models for dark matter, other d operators etc. Models  
792 that are based on Supersymmetry and not just effective theories.

793 Sätt av ett kort kapitel sist i rapporten till att avrunda och föreslå räkningar för  
794 framtida utveckling av arbetet.

795 Saving as reference. test citing as: Here we cite Duck [29] [29].

796 If the above works, remember to edit myreferences.

# Appendix



# A

---

## Datasets

800 **A.1 Background processes**

801 **A.1.1 Validation**

802 For the validation the following datasets were used, with a filter at generator level  
 803 at 450GeV for lead jet and MET.

804 mc12 157539 sherpa ct10 znunupt280 v03 mc12 157534 sherpa ct10 wenupt200  
 805 v03  
 806 mc12 157535 sherpa ct10 wmunupt200 v03  
 807 mc12 157536 sherpa ct10 wtaunupt200 v03  
 808 mc12 129160 pythia8 au2cteq6l1 perf jf17 v03  
 809 mc12 129160 pythia8 au2cteq6l1 perf jf17 v04  
 810 mc12 129170 pythia8 au2cteq6l1 gammajet dp17 v04

811 They should be read as such: Monte Carlo version, dataset number, generator, ?  
 812 name.

813 **A.1.2 Background to signals**

814 The same as the above though now with the filter as indicated by their name. The  
 815 second znunu sample has been generated with and center of mass energy at 8  
 816 TeV.

817 mc12 157539 sherpa ct10 znunupt280 v05  
 818 mc12 157539 8tev sherpa ct10 znunupt280 v05  
 819 mc12 157536 sherpa ct10 wtaunupt200 v05  
 820 mc12 157534 sherpa ct10 wenupt200 v05  
 821 mc12 157535 sherpa ct10 wmunupt200 v05

## 822 A.2 Signals

### 823 A.2.1 Qcut

824 Qcut means that the original data has been split into different parts depending  
 825 on the value of the lead jet pt.

### 826 A.2.2 D5 signal processes

```
827 mc12 188408 madgraphpythia auet2bcteq6l1 d5 dm50 ms10000 qcut200 v06
828 mc12 188409 madgraphpythia auet2bcteq6l1 d5 dm50 ms10000 qcut400 v06
829 mc12 188410 madgraphpythia auet2bcteq6l1 d5 dm50 ms10000 qcut600 v06
830 mc12 188411 madgraphpythia auet2bcteq6l1 d5 dm400 ms10000 qcut200 v06
831 mc12 188412 madgraphpythia auet2bcteq6l1 d5 dm400 ms10000 qcut400 v06
832 mc12 188413 madgraphpythia auet2bcteq6l1 d5 dm400 ms10000 qcut600 v06
```

833 All signals should be read as such: Monte Carlo version, dataset number, generator, ?, name of operator, dark matter mass, default mass suppression scale,  
 834 qcut part. As discussed in reference

### 836 A.2.3 Light vector mediator processes

```
837 mc12 188414 madgraphpythia auet2bcteq6l1 dmv dm50 mm100 w3 qcut200
838 v06
839 mc12 188422 madgraphpythia auet2bcteq6l1 dmv dm50 mm100 w3 qcut400
840 v06
841 mc12 188430 madgraphpythia auet2bcteq6l1 dmv dm50 mm100 w3 qcut600
842 v06
843 mc12 188415 madgraphpythia auet2bcteq6l1 dmv dm50 mm300 w3 qcut200
844 v06
845 mc12 188423 madgraphpythia auet2bcteq6l1 dmv dm50 mm300 w3 qcut400
846 v06
847 mc12 188431 madgraphpythia auet2bcteq6l1 dmv dm50 mm300 w3 qcut600
848 v06
849 mc12 188416 madgraphpythia auet2bcteq6l1 dmv dm50 mm500 w3 qcut200
850 v06
851 mc12 188424 madgraphpythia auet2bcteq6l1 dmv dm50 mm500 w3 qcut400
852 v06
853 mc12 188432 madgraphpythia auet2bcteq6l1 dmv dm50 mm500 w3 qcut600
854 v06
855 mc12 188417 madgraphpythia auet2bcteq6l1 dmv dm50 mm1000 w3 qcut200
856 v06
857 mc12 188425 madgraphpythia auet2bcteq6l1 dmv dm50 mm1000 w3 qcut400
858 v06
859 mc12 188433 madgraphpythia auet2bcteq6l1 dmv dm50 mm1000 w3 qcut600
860 v06
```

```
861 mc12 188418 madgraphpythia auet2bcteq6l1 dmv dm50 mm3000 w3 qcut200  
862 v06  
863 mc12 188426 madgraphpythia auet2bcteq6l1 dmv dm50 mm3000 w3 qcut400  
864 v06  
865 mc12 188434 madgraphpythia auet2bcteq6l1 dmv dm50 mm3000 w3 qcut600  
866 v06  
867 mc12 188419 madgraphpythia auet2bcteq6l1 dmv dm50 mm6000 w3 qcut200  
868 v06  
869 mc12 188427 madgraphpythia auet2bcteq6l1 dmv dm50 mm6000 w3 qcut400  
870 v06  
871 mc12 188435 madgraphpythia auet2bcteq6l1 dmv dm50 mm6000 w3 qcut600  
872 v06  
873 mc12 188420 madgraphpythia auet2bcteq6l1 dmv dm50 mm10000 w3 qcut200  
874 v06  
875 mc12 188428 madgraphpythia auet2bcteq6l1 dmv dm50 mm10000 w3 qcut400  
876 v06  
877 mc12 188436 madgraphpythia auet2bcteq6l1 dmv dm50 mm10000 w3 qcut600  
878 v06  
879 mc12 188421 madgraphpythia auet2bcteq6l1 dmv dm50 mm15000 w3 qcut200  
880 v06  
881 mc12 188429 madgraphpythia auet2bcteq6l1 dmv dm50 mm15000 w3 qcut400  
882 v06  
883 mc12 188437 madgraphpythia auet2bcteq6l1 dmv dm50 mm15000 w3 qcut600  
884 v06  
885 mc12 188438 madgraphpythia auet2bcteq6l1 dmv dm50 mm100 w8pi qcut200  
886 v06  
887 mc12 188446 madgraphpythia auet2bcteq6l1 dmv dm50 mm100 w8pi qcut400  
888 v06  
889 mc12 188454 madgraphpythia auet2bcteq6l1 dmv dm50 mm100 w8pi qcut600  
890 v06  
891 mc12 188439 madgraphpythia auet2bcteq6l1 dmv dm50 mm300 w8pi qcut200  
892 v06  
893 mc12 188447 madgraphpythia auet2bcteq6l1 dmv dm50 mm300 w8pi qcut400  
894 v06  
895 mc12 188455 madgraphpythia auet2bcteq6l1 dmv dm50 mm300 w8pi qcut600  
896 v06  
897 mc12 188440 madgraphpythia auet2bcteq6l1 dmv dm50 mm500 w8pi qcut200  
898 v06  
899 mc12 188448 madgraphpythia auet2bcteq6l1 dmv dm50 mm500 w8pi qcut400  
900 v06  
901 mc12 188456 madgraphpythia auet2bcteq6l1 dmv dm50 mm500 w8pi qcut600  
902 v06
```

```
903 mc12 188441 madgraphpythia auet2bcteq6l1 dmv dm50 mm1000 w8pi qcut200  
904 v06  
905 mc12 188449 madgraphpythia auet2bcteq6l1 dmv dm50 mm1000 w8pi qcut400  
906 v06  
907 mc12 188457 madgraphpythia auet2bcteq6l1 dmv dm50 mm1000 w8pi qcut600  
908 v06  
909 mc12 188442 madgraphpythia auet2bcteq6l1 dmv dm50 mm3000 w8pi qcut200  
910 v06  
911 mc12 188450 madgraphpythia auet2bcteq6l1 dmv dm50 mm3000 w8pi qcut400  
912 v06  
913 mc12 188458 madgraphpythia auet2bcteq6l1 dmv dm50 mm3000 w8pi qcut600  
914 v06  
915 mc12 188444 madgraphpythia auet2bcteq6l1 dmv dm50 mm10000 w8pi qcut200  
916 v06  
917 mc12 188452 madgraphpythia auet2bcteq6l1 dmv dm50 mm10000 w8pi qcut400  
918 v06  
919 mc12 188460 madgraphpythia auet2bcteq6l1 dmv dm50 mm10000 w8pi qcut600  
920 v06  
921 mc12 188445 madgraphpythia auet2bcteq6l1 dmv dm50 mm15000 w8pi qcut200  
922 v06  
923 mc12 188453 madgraphpythia auet2bcteq6l1 dmv dm50 mm15000 w8pi qcut400  
924 v06  
925 mc12 188461 madgraphpythia auet2bcteq6l1 dmv dm50 mm15000 w8pi qcut600  
926 v06  
927 mc12 188462 madgraphpythia auet2bcteq6l1 dmv dm400 mm500 w3 qcut200  
928 v06  
929 mc12 188468 madgraphpythia auet2bcteq6l1 dmv dm400 mm500 w3 qcut400  
930 v06  
931 mc12 188474 madgraphpythia auet2bcteq6l1 dmv dm400 mm500 w3 qcut600  
932 v06  
933 mc12 188463 madgraphpythia auet2bcteq6l1 dmv dm400 mm1000 w3 qcut200  
934 v06  
935 mc12 188469 madgraphpythia auet2bcteq6l1 dmv dm400 mm1000 w3 qcut400  
936 v06  
937 mc12 188475 madgraphpythia auet2bcteq6l1 dmv dm400 mm1000 w3 qcut600  
938 v06  
939 mc12 188464 madgraphpythia auet2bcteq6l1 dmv dm400 mm3000 w3 qcut200  
940 v06  
941 mc12 188470 madgraphpythia auet2bcteq6l1 dmv dm400 mm3000 w3 qcut400  
942 v06  
943 mc12 188476 madgraphpythia auet2bcteq6l1 dmv dm400 mm3000 w3 qcut600  
944 v06
```

```
945 mc12 188465 madgraphpythia auet2bcteq6l1 dmv dm400 mm6000 w3 qcut200  
946 v06  
947 mc12 188471 madgraphpythia auet2bcteq6l1 dmv dm400 mm6000 w3 qcut400  
948 v06  
949 mc12 188477 madgraphpythia auet2bcteq6l1 dmv dm400 mm6000 w3 qcut600  
950 v06  
951 mc12 188466 madgraphpythia auet2bcteq6l1 dmv dm400 mm10000 w3 qcut200  
952 v06  
953 mc12 188472 madgraphpythia auet2bcteq6l1 dmv dm400 mm10000 w3 qcut400  
954 v06  
955 mc12 188478 madgraphpythia auet2bcteq6l1 dmv dm400 mm10000 w3 qcut600  
956 v06  
957 mc12 188467 madgraphpythia auet2bcteq6l1 dmv dm400 mm15000 w3 qcut200  
958 v06  
959 mc12 188473 madgraphpythia auet2bcteq6l1 dmv dm400 mm15000 w3 qcut400  
960 v06  
961 mc12 188479 madgraphpythia auet2bcteq6l1 dmv dm400 mm15000 w3 qcut600  
962 v06  
963 mc12 188480 madgraphpythia auet2bcteq6l1 dmv dm400 mm500 w8pi qcut200  
964 v06  
965 mc12 188486 madgraphpythia auet2bcteq6l1 dmv dm400 mm500 w8pi qcut400  
966 v06  
967 mc12 188492 madgraphpythia auet2bcteq6l1 dmv dm400 mm500 w8pi qcut600  
968 v06  
969 mc12 188481 madgraphpythia auet2bcteq6l1 dmv dm400 mm1000 w8pi qcut200  
970 v06  
971 mc12 188487 madgraphpythia auet2bcteq6l1 dmv dm400 mm1000 w8pi qcut400  
972 v06  
973 mc12 188493 madgraphpythia auet2bcteq6l1 dmv dm400 mm1000 w8pi qcut600  
974 v06  
975 mc12 188482 madgraphpythia auet2bcteq6l1 dmv dm400 mm3000 w8pi qcut200  
976 v06  
977 mc12 188488 madgraphpythia auet2bcteq6l1 dmv dm400 mm3000 w8pi qcut400  
978 v06  
979 mc12 188494 madgraphpythia auet2bcteq6l1 dmv dm400 mm3000 w8pi qcut600  
980 v06  
981 mc12 188483 madgraphpythia auet2bcteq6l1 dmv dm400 mm6000 w8pi qcut200  
982 v06  
983 mc12 188489 madgraphpythia auet2bcteq6l1 dmv dm400 mm6000 w8pi qcut400  
984 v06  
985 mc12 188495 madgraphpythia auet2bcteq6l1 dmv dm400 mm6000 w8pi qcut600  
986 v06
```

```
987 mc12 188484 madgraphpythia auet2bcteq6l1 dmv dm400 mm10000 w8pi qcut200  
988 v06  
989 mc12 188490 madgraphpythia auet2bcteq6l1 dmv dm400 mm10000 w8pi qcut400  
990 v06  
991 mc12 188496 madgraphpythia auet2bcteq6l1 dmv dm400 mm10000 w8pi qcut600  
992 v06  
993 mc12 188485 madgraphpythia auet2bcteq6l1 dmv dm400 mm15000 w8pi qcut200  
994 v06  
995 mc12 188491 madgraphpythia auet2bcteq6l1 dmv dm400 mm15000 w8pi qcut400  
996 v06  
997 mc12 188497 madgraphpythia auet2bcteq6l1 dmv dm400 mm15000 w8pi qcut600  
998 v06
```

---

## Bibliography

- [1] Collaboration ATLAS. Letter of Intent for the Phase-II Upgrade of the ATLAS Experiment. Dec 2012. URL <https://cds.cern.ch/record/1502664/>. Cited on pages 1, 17, 26, and 28.
- [2] B.H. Bransden and C.J. Joachain. *Quantum mechanics*. Pearson Education, second edition, 2000. Cited on page 3.
- [3] Sven-Patrik Hallsjö. Covering the sphere with noncontextuality inequalities. Bachelor's thesis, Linköping University, The Institute of Technology, 2013. URL [http://urn.kb.se/resolve?urn=urn:nbn:se:liu:diva-103663](http://urn.kb.se/resolve?urn=urn:nbn:se:liu.diva-103663). Cited on page 3.
- [4] A. Zee. *Quantum Field Theory in a Nutshell*. Princeton University Press, illustrated edition edition, March 2003. ISBN 0691010196. Cited on pages 3, 6, and 7.
- [5] Herbert Goldstein, Charles P. Poole, and John L. Safko. *Classical Mechanics (3rd Edition)*. Addison-Wesley, 3 edition, June 2001. ISBN 0201657023. Cited on page 3.
- [6] W. E. Burcham and M. Jobes. *Nuclear and Particle Physics*. Pearson education, second edition, 1995. Cited on page 4.
- [7] The ATLAS Collaboration. Observation of a new particle in the search for the Standard Model Higgs boson with the ATLAS detector at the LHC. *Phys. Lett. B*, 716(arXiv:1207.7214). CERN-PH-EP-2012-218):1–29. 39 p, Aug 2012. Cited on page 4.
- [8] Standard model of elementary particles. [http://en.wikipedia.org/wiki/File:Standard\\_Model\\_of\\_Elementary\\_Particles.svg](http://en.wikipedia.org/wiki/File:Standard_Model_of_Elementary_Particles.svg), 2014. Accessed: 2014-03-24. Cited on page 4.
- [9] G. Jungman, M. Kamionkowski, and K. Griest. Supersymmetric dark matter. *Physics Reports*, 267:195–373, March 1996. doi: 10.1016/0370-1573(95)00058-5. Cited on pages 4 and 5.

- 1028 [10] NASA. NASA's solar system exploration: the planets: orbits and  
1029 physical characteristics. <https://solarsystem.nasa.gov/planets/>  
1030 charchart.cfm, 2014. Accessed: 2014-03-21. Cited on page 6.
- 1031 [11] T. S. van Albada, J. N. Bahcall, K. Begeman, and R. Sancisi. Distribution  
1032 of dark matter in the spiral galaxy NGC 3198. *Astrophysical Journal*, 295:  
1033 305–313, August 1985. doi: 10.1086/163375. Cited on page 6.
- 1034 [12] Jessica Goodman, Masahiro Ibe, Arvind Rajaraman, William Shepherd,  
1035 Tim M.P. Tait, et al. Constraints on Light Majorana dark Matter from Collid-  
1036 ers. *Phys.Lett.*, B695:185–188, 2011. doi: 10.1016/j.physletb.2010.11.009.  
1037 Cited on pages 5 and 7.
- 1038 [13] ATLAS Collaboration. Search for dark matter candidates and large extra di-  
1039 mensions in events with a jet and missing transverse momentum with the at-  
1040 las detector. *J. High Energy Phys.*, 04(arXiv:1210.4491. CERN-PH-EP-2012-  
1041 210):075. 58 p, October 2012. URL [http://cds.cern.ch/record/](http://cds.cern.ch/record/1485031)  
1042 1485031. Cited on pages 5, 8, and 9.
- 1043 [14] J. Goodman, M. Ibe, A. Rajaraman, W. Shepherd, T. M. P. Tait, and H.-B. Yu.  
1044 Constraints on dark matter from colliders. *Phys.Rev.D82:116010,2010*, 82  
1045 (11):116010, December 2010. doi: 10.1103/PhysRevD.82.116010. Cited on  
1046 page 7.
- 1047 [15] ATLAS. Atlas luminosity public results. <https://twiki.cern.ch/twiki/bin/view/AtlasPublic/LuminosityPublicResults>, 2013.  
1048 Accessed: 2014-03-06. Cited on page 10.
- 1049 [16] AC Team. The four main LHC experiments, Jun 1999. URL <http://cds.cern.ch/record/40525>. Cited on page 10.
- 1050 [17] Werner Herr and B Muratori. Concept of luminosity. 2006. URL <http://cds.cern.ch/record/941318/>. Cited on page 11.
- 1051 [18] The ATLAS Collaboration. The atlas experiment at the cern large hadron col-  
1052 linder. *Journal of Instrumentation*, 3(08):S08003. 437 p, 2008. URL <https://cdsweb.cern.ch/record/1129811/>. Cited on pages 11 and 12.
- 1053 [19] Joao Pequenao. Computer generated image of the whole ATLAS detector,  
1054 Mar 2008. URL <http://cds.cern.ch/record/1095924>. Cited on page  
1055 12.
- 1056 [20] ATLAS Collaboration. Event display for one of the monojet candidates in  
1057 the data. The event has a jet with  $\text{pt} = 602 \text{ GeV}$  at  $\eta = -1$  and  $\phi =$   
1058  $2.6$ ,  $\text{MET} = 523 \text{ GeV}$ , and no additional jet with  $\text{pt}_{\text{jet}} > 30 \text{ GeV}$  in the fi-  
1059 nal state.. [https://atlas.web.cern.ch/Atlas/GROUPS/PHYSICS/](https://atlas.web.cern.ch/Atlas/GROUPS/PHYSICS/CONFNOTES/ATLAS-CONF-2011-096/fig_08.png)  
1060 [CONFNOTES/ATLAS-CONF-2011-096/fig\\_08.png](https://atlas.web.cern.ch/Atlas/GROUPS/PHYSICS/CONFNOTES/ATLAS-CONF-2011-096/fig_08.png), 2011. Accessed:  
1061 2014-03-28. Cited on page 13.
- 1062 [21] ATLAS Collaboration. Physics at a High-Luminosity LHC with ATLAS. Jul  
1063

- 1067        2013. URL <https://cds.cern.ch/record/1564937>. Cited on page  
1068        15.
- 1069 [22] J. Alwall, M. Herquet, F. Maltoni, O. Mattelaer, and T. Stelzer. MadGraph  
1070        5: going beyond. *Journal of High Energy Physics*, 6:128, June 2011. doi:  
1071        10.1007/JHEP06(2011)128. Cited on page 15.
- 1072 [23] Torbjörn Sjöstrand, Stephen Mrenna, and Peter Skands. A brief introduc-  
1073        tion to {PYTHIA} 8.1. *Computer Physics Communications*, 178(11):852 –  
1074        867, 2008. ISSN 0010-4655. doi: [http://dx.doi.org/10.1016/j.cpc.2008.  
1075        01.036](http://dx.doi.org/10.1016/j.cpc.2008.01.036). URL [http://www.sciencedirect.com/science/article/  
1076        pii/S0010465508000441](http://www.sciencedirect.com/science/article/pii/S0010465508000441). Cited on page 15.
- 1077 [24] The ROOT Team. Root. <http://root.cern.ch/drupal/>, 2014. Ac-  
1078        cessed: 2014-03-28. Cited on page 15.
- 1079 [25] S. Agostinelli, J. Allison, K. Amako, J. Apostolakis, H. Araujo, P. Arce,  
1080        M. Asai, D. Axen, S. Banerjee, G. Barrand, F. Behner, L. Bellagamba,  
1081        J. Boudreau, L. Broglia, A. Brunengo, H. Burkhardt, S. Chauvie, J. Chuma,  
1082        R. Chytracek, G. Cooperman, G. Cosmo, P. Degtyarenko, A. Dell'Acqua,  
1083        G. Depaola, D. Dietrich, R. Enami, A. Feliciello, C. Ferguson, H. Fe-  
1084        sefeldt, G. Folger, F. Foppiano, A. Forti, S. Garelli, S. Giani, R. Gi-  
1085        annitrapani, D. Gibin, J.J. Gómez Cadenas, I. González, G. Gracia  
1086        Abril, G. Greeniaus, W. Greiner, V. Grichine, A. Grossheim, S. Guatelli,  
1087        P. Gumligner, R. Hamatsu, K. Hashimoto, H. Hasui, A. Heikkinen,  
1088        A. Howard, V. Ivanchenko, A. Johnson, F.W. Jones, J. Kallenbach, N. Kanaya,  
1089        M. Kawabata, Y. Kawabata, M. Kawaguti, S. Kelner, P. Kent, A. Kimura,  
1090        T. Kodama, R. Kokoulin, M. Kossov, H. Kurashige, E. Lamanna, T. Lampén,  
1091        V. Lara, V. Lefebure, F. Lei, M. Liendl, W. Lockman, F. Longo, S. Magni,  
1092        M. Maire, E. Medernach, K. Minamimoto, P. Mora de Freitas, Y. Morita,  
1093        K. Murakami, M. Nagamatu, R. Nartallo, P. Nieminen, T. Nishimura, K. Oht-  
1094        subo, M. Okamura, S. O'Neale, Y. Oohata, K. Paech, J. Perl, A. Pfeiffer,  
1095        M.G. Pia, F. Ranjard, A. Rybin, S. Sadilov, E. Di Salvo, G. Santin, T. Sasaki,  
1096        N. Savvas, Y. Sawada, S. Scherer, S. Sei, V. Sirotenko, D. Smith, N. Starkov,  
1097        H. Stoecker, J. Sulkimo, M. Takahata, S. Tanaka, E. Tcherniaev, E. Safai  
1098        Tehrani, M. Tropeano, P. Truscott, H. Uno, L. Urban, P. Urban, M. Verderi,  
1099        A. Walkden, W. Wander, H. Weber, J.P. Wellisch, T. Wenaus, D.C. Williams,  
1100        D. Wright, T. Yamada, H. Yoshida, and D. Zschiesche. Geant4—a sim-  
1101        ulation toolkit. *Nuclear Instruments and Methods in Physics Research  
1102        Section A: Accelerators, Spectrometers, Detectors and Associated Equipment*,  
1103        506(3):250 – 303, 2003. ISSN 0168-9002. doi: [http://dx.doi.org/  
1104        10.1016/S0168-9002\(03\)01368-8](http://dx.doi.org/10.1016/S0168-9002(03)01368-8). URL <http://www.sciencedirect.com/science/article/pii/S0168900203013688>. Cited on page 17.
- 1105 [26] ATLAS Collaboration. Performance assumptions for an upgraded ATLAS  
1106        detector at a High-Luminosity LHC. Mar 2013. URL [https://cds.cern.  
1107        ch/record/1527529/](https://cds.cern.ch/record/1527529/). Cited on pages 17, 20, 26, 27, and 28.
- 1108 [27] ATLAS Collaboration. Electron performance measurements with the ATLAS

1110 detector using the 2010 LHC proton-proton collision data. *Eur. Phys. J. C*,  
1111 72(arXiv:1110.3174. CERN-PH-EP-2011-117):1909. 45 p, Oct 2011. Com-  
1112 ments: 33 pages plus author list (45 pages total), 24 figures, 12 tables, sub-  
1113 mitted to Eur. Phys. J. C. Cited on pages 26 and 28.

1114 [28] ATLAS Collaboration. Search for New Phenomena in Monojet plus Missing  
1115 Transverse Momentum Final States using 10fb-1 of pp Collisions at  $\sqrt{s}=8$   
1116 TeV with the ATLAS detector at the LHC. Nov 2012. URL [http://cds.  
1117 cern.ch/record/1493486/](http://cds.cern.ch/record/1493486/). Cited on pages 32, 34, 35, and 36.

1118 [29] Donald Duck. The history of automatic control. *Duckburg Journal of Sci-  
1119 ence*, 106(3):345–401, 2005. Cited on page 46.

1121 **Upphovsrätt**

1122 Detta dokument hålls tillgängligt på Internet — eller dess framtida ersättare —  
 1123 under 25 år från publiceringsdatum under förutsättning att inga extraordinära  
 1124 omständigheter uppstår.

1125 Tillgång till dokumentet innebär tillstånd för var och en att läsa, ladda ner,  
 1126 skriva ut enstaka kopior för enskilt bruk och att använda det oförändrat för icke-  
 1127 kommersiell forskning och för undervisning. Överföring av upphovsrätten vid  
 1128 en senare tidpunkt kan inte upphäva detta tillstånd. All annan användning av  
 1129 dokumentet kräver upphovsmannens medgivande. För att garantera äktheten,  
 1130 säkerheten och tillgängligheten finns det lösningar av teknisk och administrativ  
 1131 art.

1132 Upphovsmannens ideella rätt innehåller rätt att bli nämnd som upphovsman  
 1133 i den omfattning som god sed kräver vid användning av dokumentet på ovan  
 1134 beskrivna sätt samt skydd mot att dokumentet ändras eller presenteras i sådan  
 1135 form eller i sådant sammanhang som är kränkande för upphovsmannens litterära  
 1136 eller konstnärliga anseende eller egenart.

1137 För ytterligare information om Linköping University Electronic Press se för-  
 1138 lagets hemsida <http://www.ep.liu.se/>

1139 **Copyright**

1140 The publishers will keep this document online on the Internet — or its possi-  
 1141 ble replacement — for a period of 25 years from the date of publication barring  
 1142 exceptional circumstances.

1143 The online availability of the document implies a permanent permission for  
 1144 anyone to read, to download, to print out single copies for his/her own use and  
 1145 to use it unchanged for any non-commercial research and educational purpose.  
 1146 Subsequent transfers of copyright cannot revoke this permission. All other uses  
 1147 of the document are conditional on the consent of the copyright owner. The  
 1148 publisher has taken technical and administrative measures to assure authenticity,  
 1149 security and accessibility.

1150 According to intellectual property law the author has the right to be men-  
 1151 tioned when his/her work is accessed as described above and to be protected  
 1152 against infringement.

1153 For additional information about the Linköping University Electronic Press  
 1154 and its procedures for publication and for assurance of document integrity, please  
 1155 refer to its www home page: <http://www.ep.liu.se/>